Henry Ford
Health System

RADIOLOGY RESEARCH

Anode/Filter Combinations in Digital Mammography

Michael Flynn
Dept. of Radiology
mikef@rad.hfh.edu

20 years ago screen-film mammography was usually performed using Mo filter Mo anode x-ray sources as recommended by NCRP 85.

Mammography, A Users Guide;
NCRP Report No. 85, 1986

In 1989, Kimme-Smith considered the contrast and the dose associated with screen film mammograms from Mo vs W anodes.

- Mo anode, 0.030 mm Mo filter
- W anode, 0.060 mm Mo filter

- At the same kVp, 27, the W anode images lacked contrast.
- Equivalent contrast was found in the W anode kVp was reduced to 23 kVp, but increased exposure was required

Film-screen mammography x-ray tube anodes: Molybdenum versus tungsten;
C Kimme-Smith, L Bassett, R Gold; , Med Phys 16 (2) 1989.

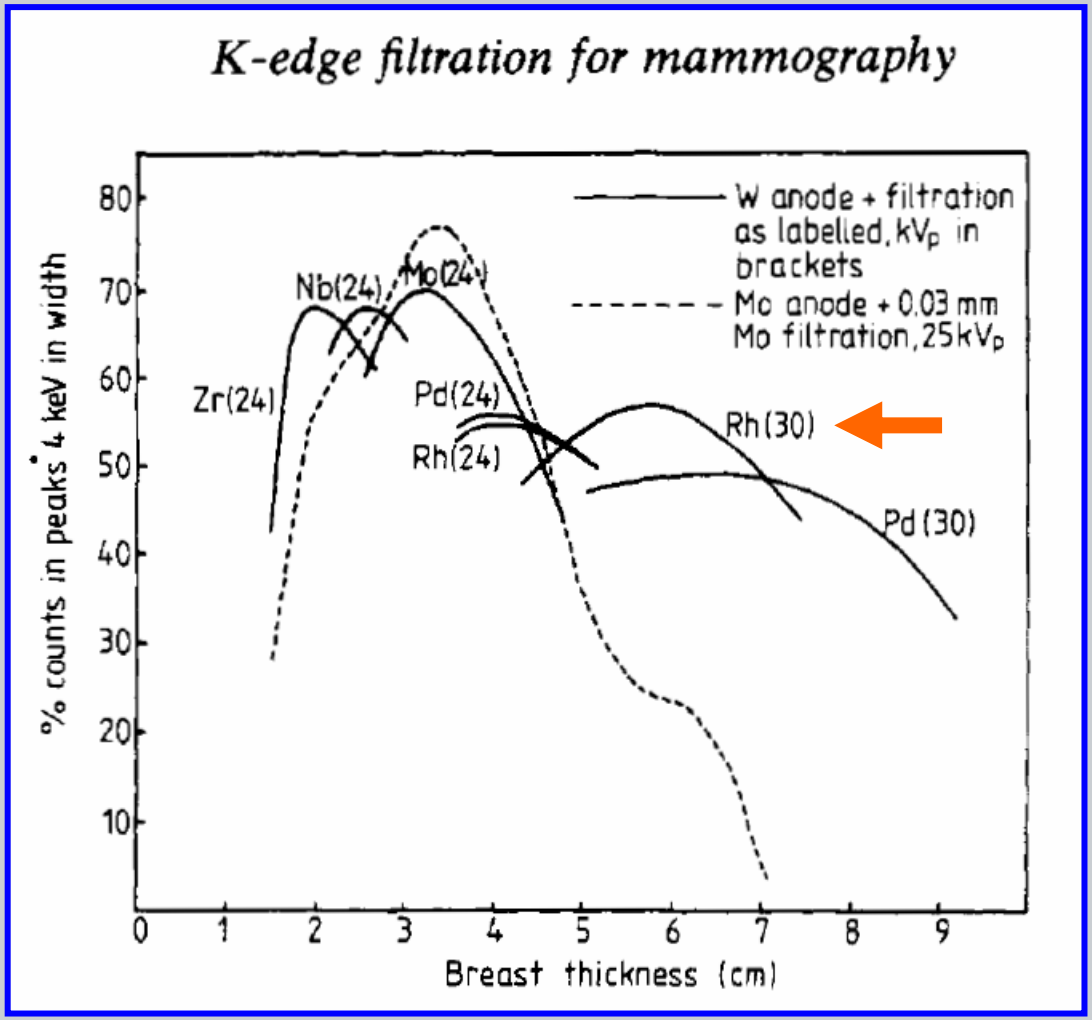

McDonagh had previously (1984) considered W anodes with K-edge filters, but had not directly assessed contrast or noise.

Optimum x-ray spectra for mammography: choice of K-edge filters for tungsten anode tubes; C McDonagh, J Leake S Beaman; Phys Med Biol 29 (3) 1984.

In 1993, Jennings reported a computation method to assess dose normalized signal to noise ratio.

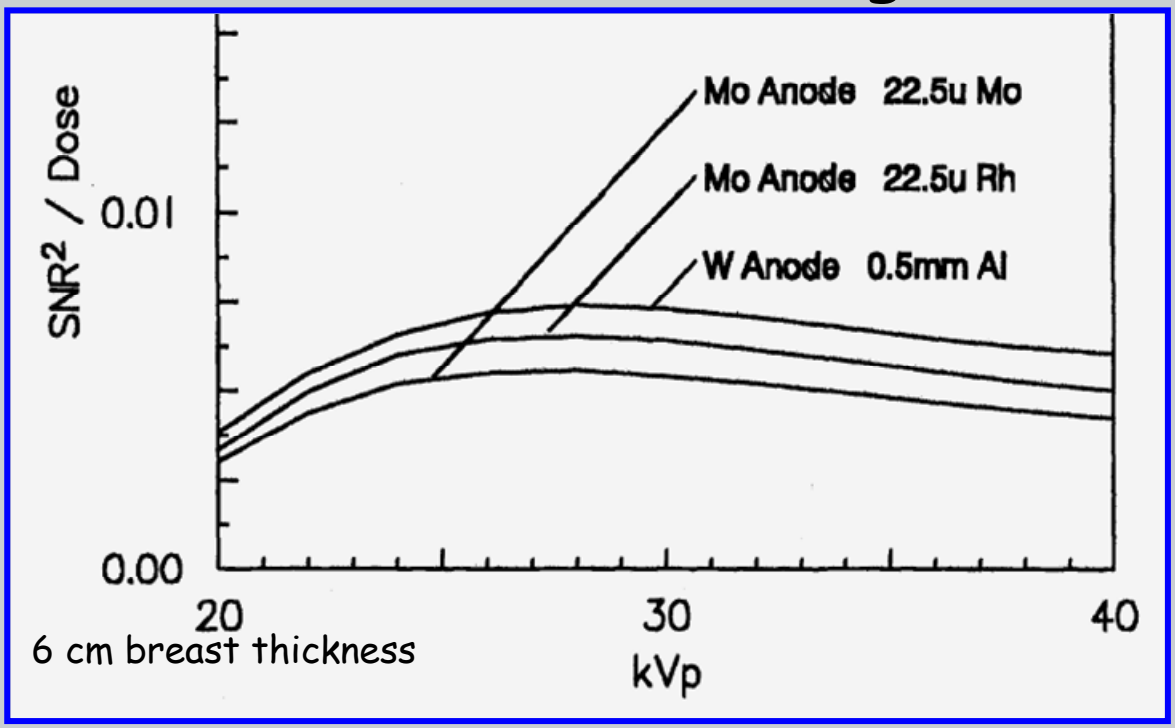

The results showed improved SNR^2/D for thick breasts with Mo/Rh.

However, image contrast was not considered.

Signal and noise properties from Nishikawa's measures (Med Phys 1985) on Min-R film screen recordings. Dose from Dance (PMB 1992)

Evaluation of x-ray sources for mammography;
R Jennings, P Quinn, T Fewell; SPIE v1896, 1993.

In 1997, Andre considered W anodes with K-edge filters for a CsI-CCD (Trex) digital receptor.

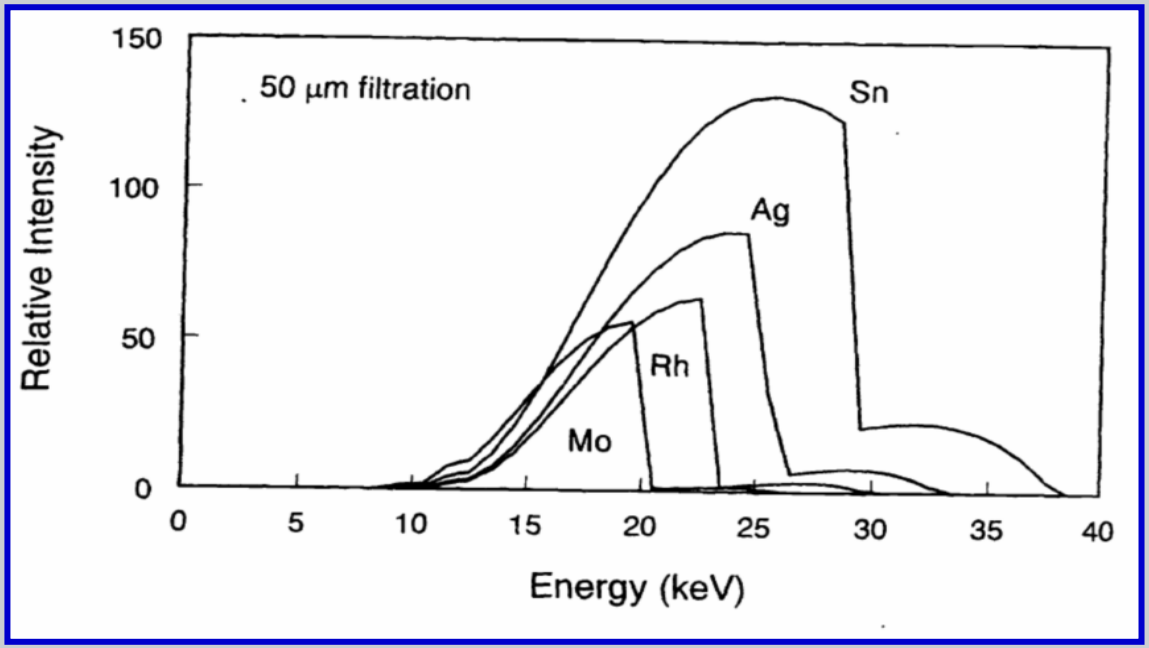

Using an approximate model, the results showed improved SNR^2/D for brems spectra with K edge filters.

<4 cm breast – 26 kVp, Mo filter
4-6 cm breast – 33 kVp, Ag filter
>6 cm breast – 38 kVp, Sn filter

Optimization of tungsten x-ray spectra for digital mammography; M Andre, B Spivey; SPIE v3032, 1997.

- In a 1999 editorial, Kimme-Smith pointed out that new digital mammography detectors may provide optimal results with different spectra than have been used with screen film systems.

  New digital mammography systems may require different x-ray spectra and, therefore, more generalized glandular dose values (editorial); C Kimme-Smith,

  Radiology 213 (1), 1999.

- The for breast dose data suitable for a broad range of spectral conditions was emphasized and Boone's report in the same issue was used as an example.

  Glandular breast dose for monoenergetic and high energy xray beams: Monte Carlo assessment; J Boone,

  Radiology 213 (1), 1999.

In this presentation, I will explain how simulation models using tables computed with Monte Carlo radiation transport analysis are used to optimize a digital mammography systems with respect to image quality in relation to absorbed breast dose. The simulation results will then be related to recent reports associated with new commercial systems.

The educational objectives are:

I. Explain the rationale for a dose normalized CNR

II. Describe computer simulation methods to simulate mammography x-ray spectra and optimize anode/filter combinations.

III. Review recent results on alternative anode/filter combinations for commercial digital mammography.

- I -

The framework for considering signal, noise and contrast in radiographic imaging systems can be appreciated from an analysis of an ideal detector system.

For an incident x-ray beam for which all x-rays have the same energy, i.e. monoenergetic, the integral expressions for the signal of a counting and of an energy integrating detector reduce to;

$$S_c = (A_d t \phi_E) \qquad S_e = E(A_d t \phi_E)$$

The expression in parenthesis, $(A_d t \phi_E)$, is just the number of photons incident on a detector element in the time t.

The noise for the counting detector signal is thus just the square root of this expression. For the energy integrating type of device, the noise is weighted by the energy term;

$$\sigma_c = (A_d t \phi_E)^{1/2} \qquad \sigma_e = E(A_d t \phi_E)^{1/2}$$

It is common to relate the amplitude of the signal to that of the noise. The signal to noise ratio, SNR, is high for images with low relative noise.

$$\frac{S_c}{\sigma_c} = (A_d t \phi_E)^{1/2} \qquad \frac{S_e}{\sigma_e} = (A_d t \phi_E)^{1/2}$$

For monoenergetic x-rays, the SNR for an ideal energy integrating detector is independent of energy and identical to that of a counting detector. The square of the signal to noise ratio is thus equal to the detector element area time the incident fluence, Φ .

$$\left(\frac{S}{\sigma}\right)^2 = A_d \Phi$$

For actual detectors recording a spectrum of radiation, the actual SNR^2 is often related to the equivalent number of mono energetic photons that would produce the same SNR with an ideal detector.

Noise Equivalent Quanta (NEQ), Φ_{eq} .

For an ideal counting detector, the signal to noise ratio for a spectrum of radiation is essential the same as for a monoenergetic beam.

$$\frac{S_c}{\sigma_c} = (A_d t \phi)^{1/2} \qquad \phi = \int_0^{E_{\max}} \phi_{(E)} dE$$

For an ideal energy integrating detector, the signal to noise ratio for a spectrum of radiation is more complicated because of the way the energy term influences the signal and the noise integrals.

First, the signal is given by the first moment integral of the differential fluence spectrum;

$$S_e = A_d t \int_0^{E_{\max}} E \phi_{(E)} dE$$

The corresponding integral expression for the noise of the signal is the second moment integral of the differential energy fluence.

$$\sigma_e^2 = A_d t \int_0^{E_{\max}} E^2 \phi_{(E)} dE$$

The corresponding integral expression for the noise of the signal is the second moment integral of the differential energy fluence.

$$\left(\frac{S_e}{\sigma_e}\right)^2 = A_d t \left[\frac{\left(\int_0^{E_{\max}} E\phi_{(E)} dE\right)^2}{\int_0^{E_{\max}} E^2 \phi_{(E)} dE}\right] = A_d \Phi_{eq}$$

In this case, the noise equivalent quanta, Φ_{eq} in photons/mm^2, is given by the ratio of the 1st moment squared to the second moment times the exposure time. The noise power spectra, NPS, is related to $1/\Phi_{eq}$ with units of mm^2.

I – Signal difference to noise ratio

The visibility of small signal changes depends on the relative signal change in relation to the signal noise

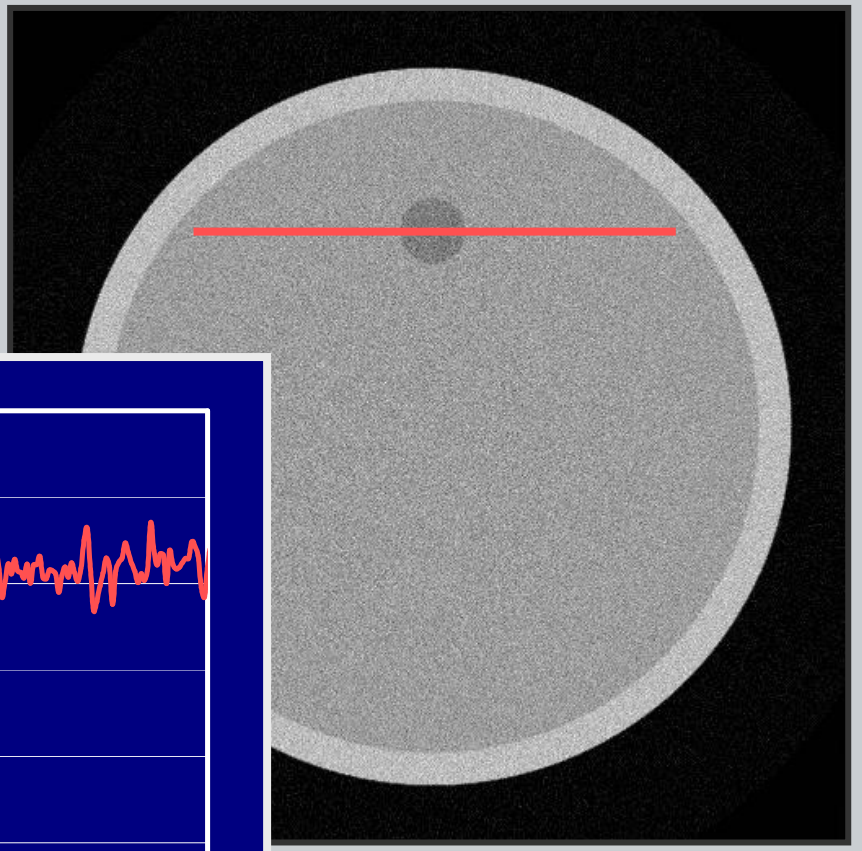

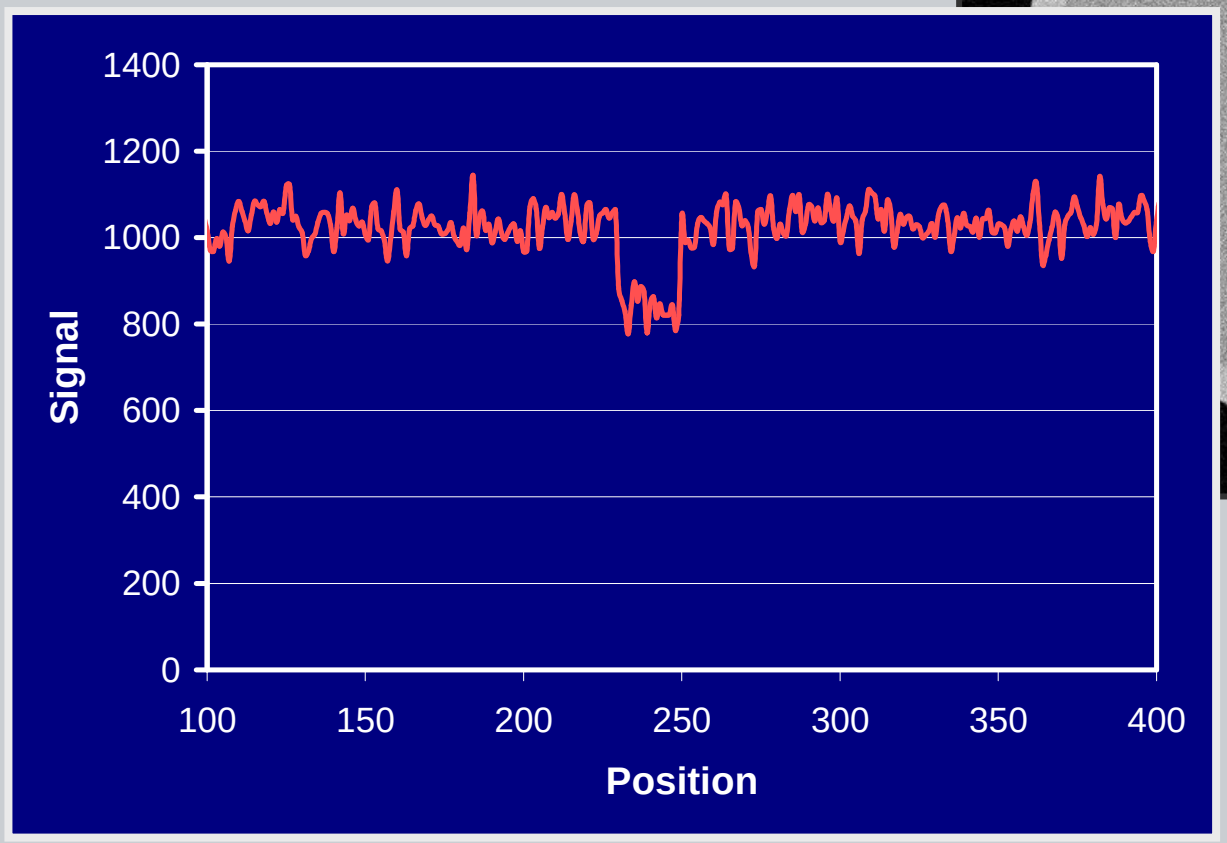

I – Signal difference, contrast and relative contrast

The relative contrast of a target structure is defined as the signal difference between the target and the background divided by the background signal.

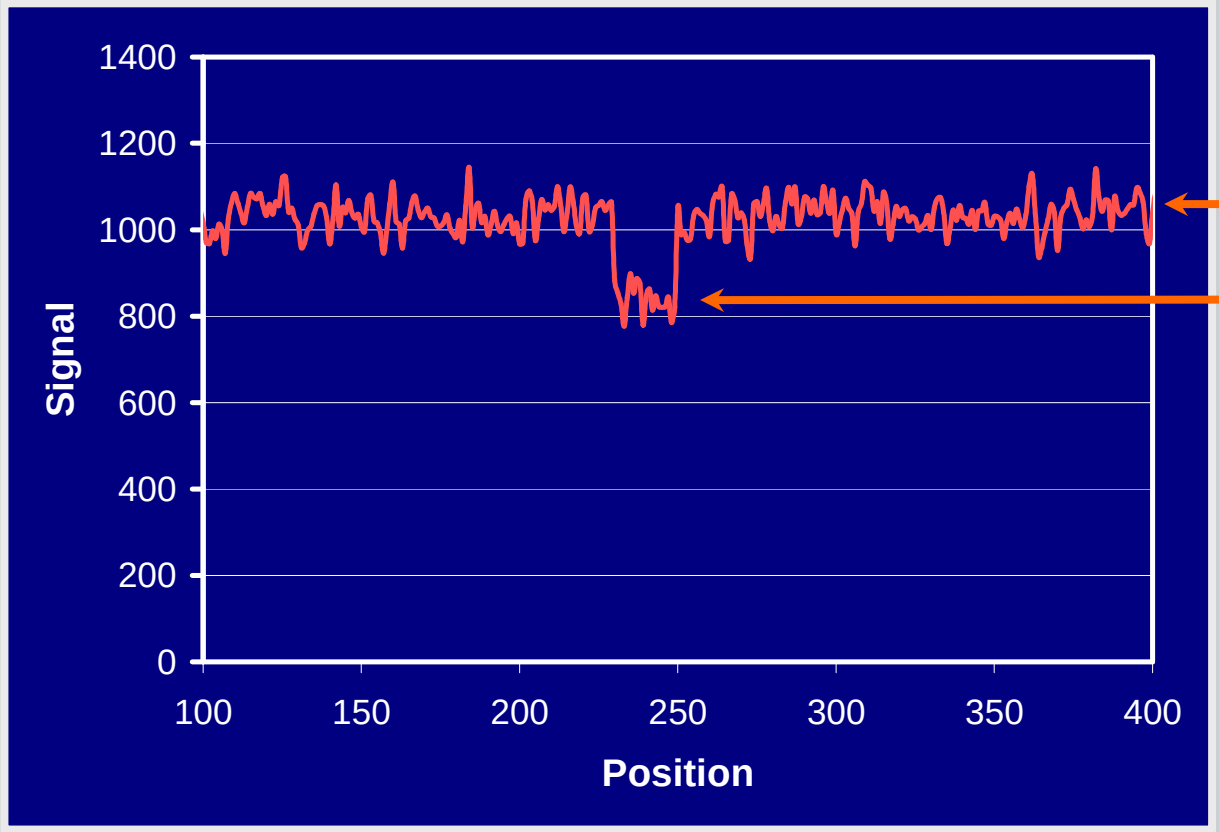

Sb

St

Contrast

$C = St - Sb$

Relative Contrast

$C_r = (St-Sb)/Sb$

Contrast to Noise Ratio

CNR

The ability to detect a small target structure of a particular size is determined by the ratio of the contrast, (St-Sb), in relation to the signal noise. CNR is equal to the product of the relative contrast and SNR.

$$\frac{C}{\sigma} = \frac{S_t - S_b}{\sigma_b} = C_r \frac{S_b}{\sigma_b}$$

I – Visibility and the Rose CNR relation

Rose showed that targets are visible if CNR adjusted for target area is larger than ~4.

S/N – For a target of area A_t, the SNR associated with quantum mottle is related to the noise equivalent quanta, Φ_{eq}.

$$\frac{\text{Signal}}{\text{Noise}} = \frac{S}{N} = \left(A_t \Phi_{eq}\right)^{1/2}$$

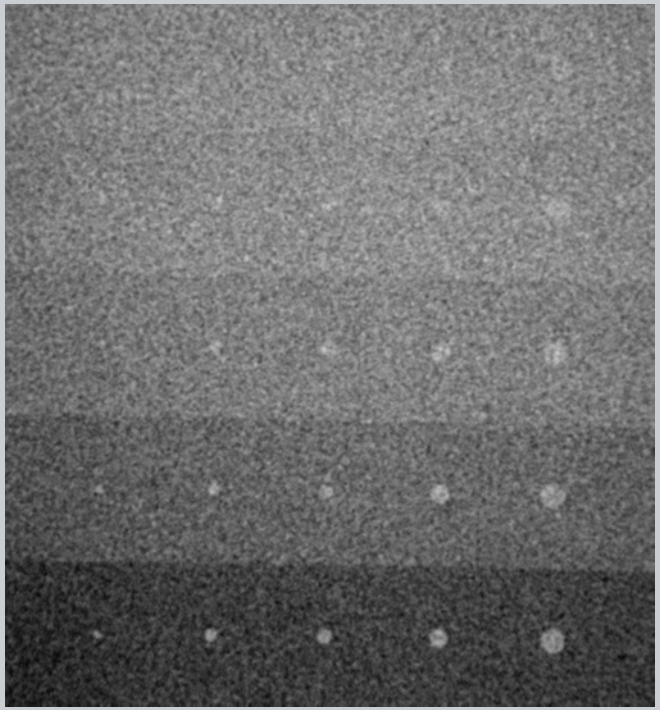

C/N – CNR is simply the product of the relative contrast and the background SNR.

$$\frac{\text{Contrast}}{\text{Noise}} = C_r \frac{S}{N} = C_r \left(A_t \Phi_{eq}\right)^{1/2}$$

Rose A, Vision – Human and Electronic, Plenum Press,

Dose Normalized Contrast to Noise Ratio

$(CNR)^2$

The square of the contrast to noise ratio is proportional to the equivalent number of detected x-ray quanta and thus proportional to mA-s

$(CNR)^2$ / *Dose*

Since the absorbed dose in the subject is also proportional to mA-s, the ratio of contrast to noise squared to absorbed dose is a logical figure of merit for optimization.

$$CNR^2/(mGy) \quad \text{or} \quad CNR/(mGy)^{1/2}$$

I – Small perturbation contrast

- Consider an analysis with the following approximations:
  - homogenous object of uniform thickness, t
  - A small cubic material perturbation, δ_t .
  - An ideal energy integrating detector
  - A mono-energetic x-ray beam.
- The relative contrast produced by a small target object results from the difference between the linear attenuation coefficient of the target material, μ_t , and that for the surrounding material, μ_b , which produces the background signal.
- The relationships for the target signal, St, and the background signal, Sb, can be written in terms of the fluence incident on the object.
- The relative contrast is thus;

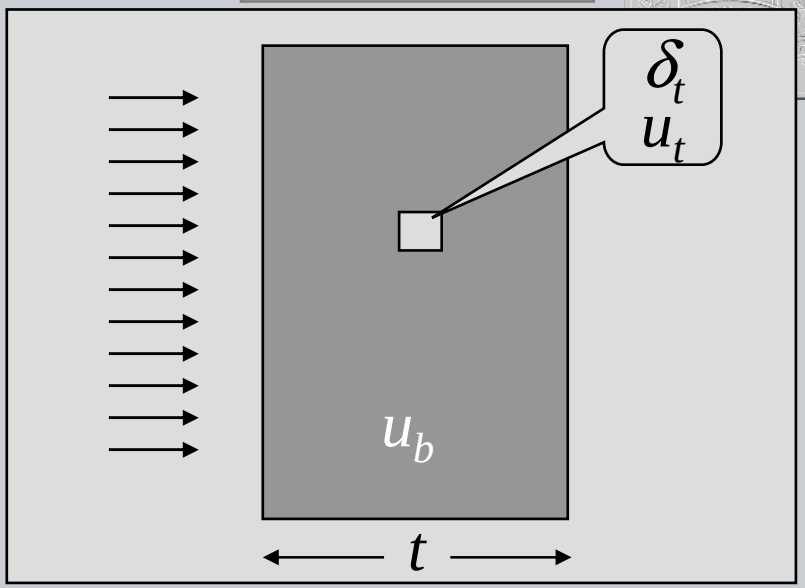

$$S_b = EA_d\Phi_o e^{-\mu_b t}$$

$$S_t = EA_d\Phi_o e^{-\mu_b(t-\delta_t)}e^{-\mu_t\delta_t}$$

$$S_t = \left(EA_d\Phi_o e^{-\mu_b t}\right)e^{-(\mu_t-\mu_b)\delta_t}$$

$$S_t = S_b e^{-(\mu_t-\mu_b)\delta_t}$$

$$C_r = \frac{S_t - S_b}{S_b} = e^{-(u_t-u_b)\delta_t} \cong -\Delta\mu\delta_t$$

- The noise variance of the signal in the background can be derived from the background signal equation using the prior results for the propogation of error.
- The noise results from the number of x-ray quanta detected, $A_d\Phi_o e^{-u_b t}$, and the energy per quanta, E , is a constant.
- Using the prior expression for the background signal, Sb , the signal to noise ratio may be easily deduced.
- The contrast to noise ratio is then simply obtained by multiplying the SNR by the relative contrast derived on the previous page.

$$\sigma_{S_b}^2 = E^2\left(A_d\Phi_o e^{-\mu_b t}\right)$$

$$\sigma_{S_b} = E\left(A_d\Phi_o\right)^{1/2} e^{-\frac{\mu_b t}{2}}$$

$$\frac{S_b}{\sigma_{S_b}} = \frac{\left(E\left(A_d\Phi_o\right)e^{-\mu_b t}\right)}{\left(E\left(A_d\Phi_o\right)^{1/2} e^{-\frac{\mu_b t}{2}}\right)}$$

$$\frac{S_b}{\sigma_{S_b}} = \left(A_d\Phi_o\right)^{1/2} e^{-\frac{\mu_b t}{2}}$$

$$\frac{C}{\sigma_{S_b}} = -\Delta\mu\delta_t\left(A_d\Phi_o\right)^{1/2} e^{-\frac{\mu_b t}{2}}$$

I – Optimal CNR

Recalling that the attenuation coefficients are strong functions of x-ray energy, $\mu(E)$ can be considered as a variable. CNR for a small void is then of the form, $CNR = kX\ exp(-Xt/2)$ where $X = \mu(E)$ (void) .

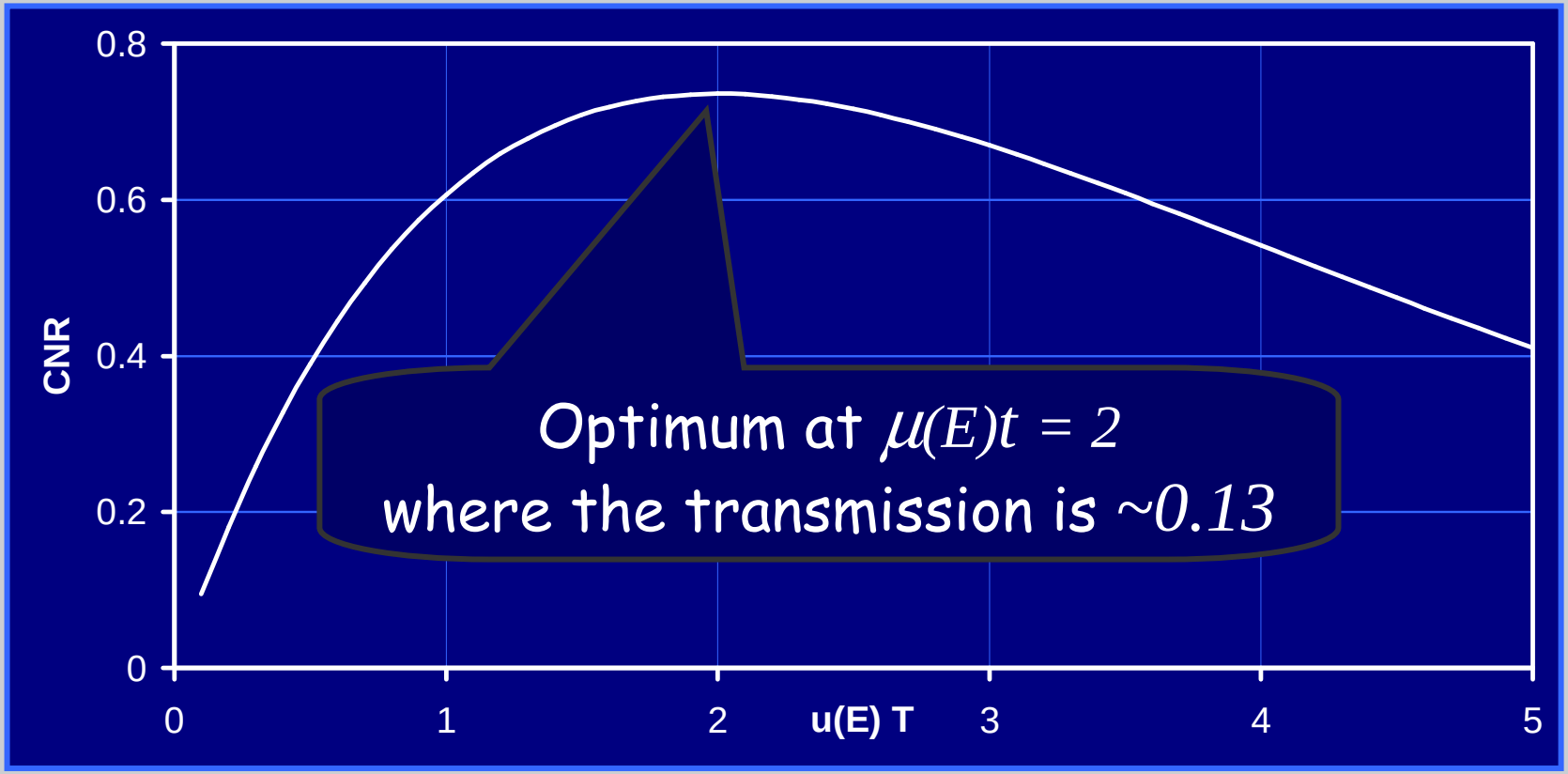

A rule of thumb based on this approximate solution says that optimal radiographs are obtained with about 10-15 percent transmission thru the object.

- II -

Anode/Filter combinations that optimize this FOM can be assessed using accurate computational models based on Monte Carlo data for dose and detector CNR.

Optimal radiographic techniques for digital mammograms obtained with an amorphous selenium detector;
M Flynn, C Dodge, D Peck, A Swinford; SPIE v5030, 2003.

II – XSPECT

XSPECT is a collection of programs that simulate the production, attenuation, and detection of x-rays in order to describe the performance of radiation imaging systems.

- **X-ray Spectrum:** The spectral distribution of the source is generated using computer models for electron target tubes or can be input from previously stored tabular data.
- **Material Attenuation:** Energy dependant spectral attenuation is computed from libraries having data on material composition and x-ray interaction coefficients.
- **Exposure:** Utility programs allow the spectra to be integrated or the determination of exposure(i.e. air ionization).
- **Dose:** Evaluation of absorbed dose from pre-computed tabulated data specific to a particular object geometry.
- **Contrast and Noise:** From pre-computed tables of signal and noise detection efficiency, the response of a particular detector system can be computed.

http://www.engin.umich.edu/class/ners580/

XSPECT BACKGROUND:

- The programs for XSPECT version 3.5 have evolved from software developments begun in 1983 in the X-ray Imaging Research Laboratory at HFHS.
- Contributions to this effort have come from Michael Flynn, Scott Wilderman, Zhiheng Ge, James Pipe, Sean Hames, Charles Dodge.
- XSPECT is now used at the core software for a Computational Laboratory course at the University of Michgan (NERS-580/BIOE-580).
- Particular recognition must be given to the efforts of Scott Wilderman who wrote the majority of the original code, assembled the initial database of interaction cross sections, and modified his Monte Carlo code, SKEPTIC, to deduce detector and dose tables.
- A major revision, version 4.0, is now in beta test.

http://www.engin.umich.edu/class/ners580/

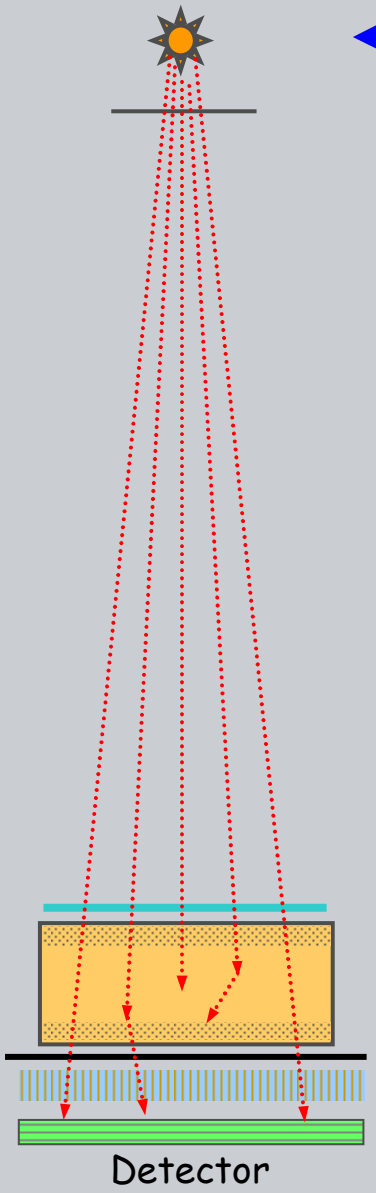

- xSpect spect_gen script call
  - Storm bremsstrahlung model
  - Self abs. based on tabata range
  - Z dependant characteristic model
- Validation
  - Tungsten – Fewell
  - Molybdenum - Boone (Jennings)

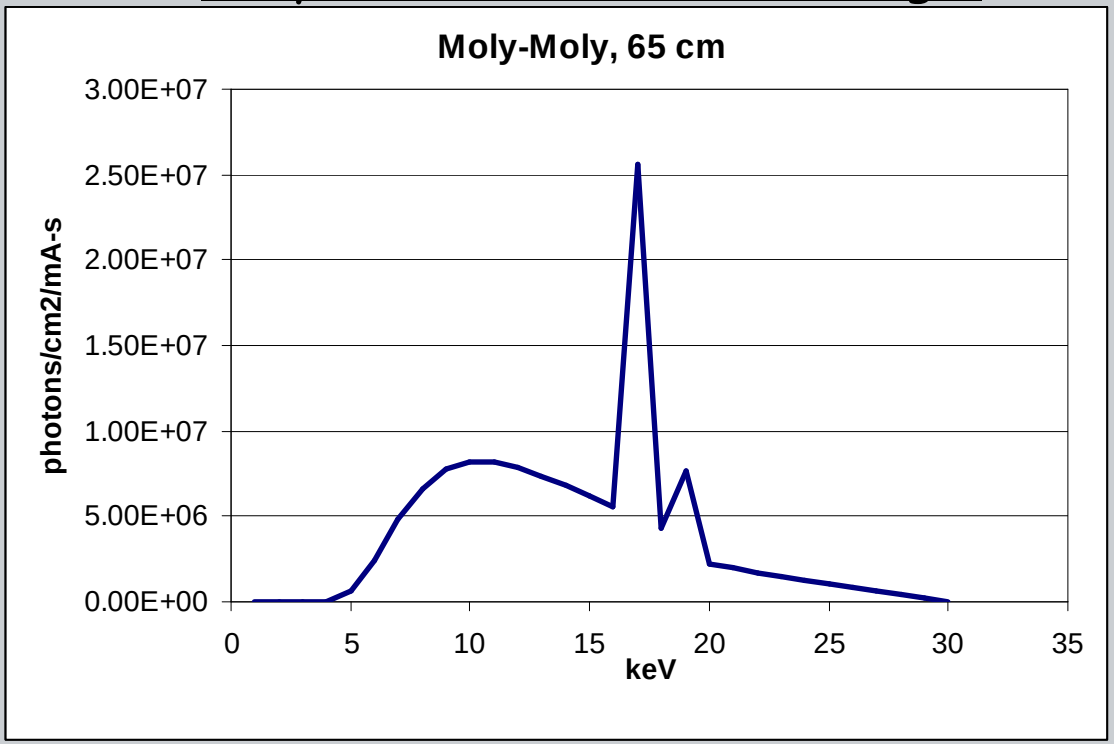

II – Spect_gen Spectra Format

X-ray spectra are stored in a standard data structure that is read or modified by various program routines.

A text structure is used so that the spectrum can be passed to procedures as a script variable or plotted.

Z angle waveform kVp

Npts dkeV distance

Ergs:photons per sr:cm^2
1 1 - ergs/(mAs-sr-keV)
1 2 - ergs/(mAs-cm^2-keV)
2 1 - xrays/(mAs-sr-keV)
2 2 - xrays/(mAs-cm^2-keV)

Conversion Utilities:
sr2cm cm2sr
cm2cm
erg2no no2erg

```
# spect_gen: 42  12.000  1  50.00
#    99   0.5000       0.0000
#    2   1  (unit flags)
#  Energy      ergs/mAs-sr-keV
    1.000          0.0000E+00
    1.500          0.0000E+00
    2.000          1.4350E-09
    2.500          1.9378E-04
       .
       .
       .
   49.500            1.6423E+01
   50.000          0.0000E+00
```

II – XSPECT spectgen-I vs Penelope MC

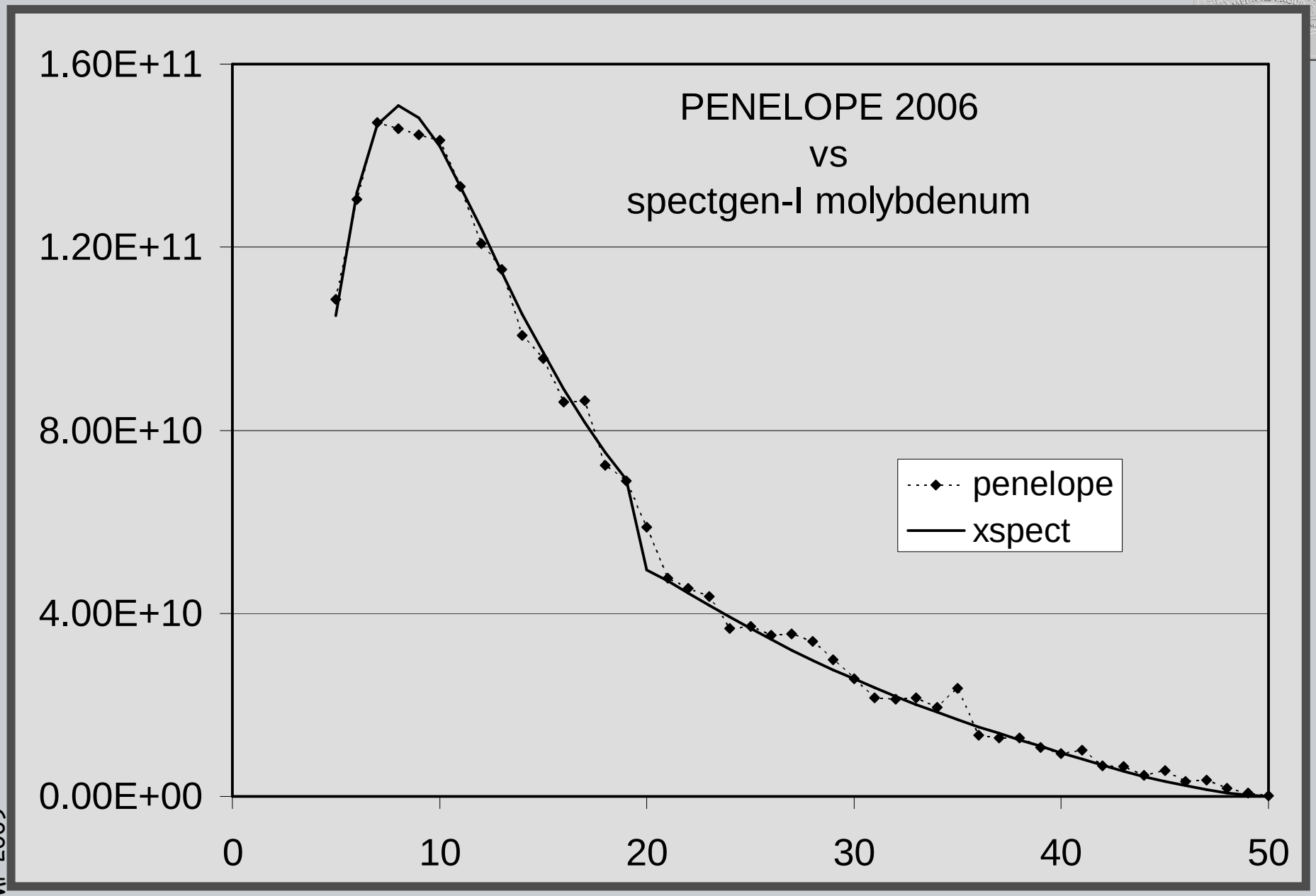

II – XSPECT spectgen-I vs Penelope MC

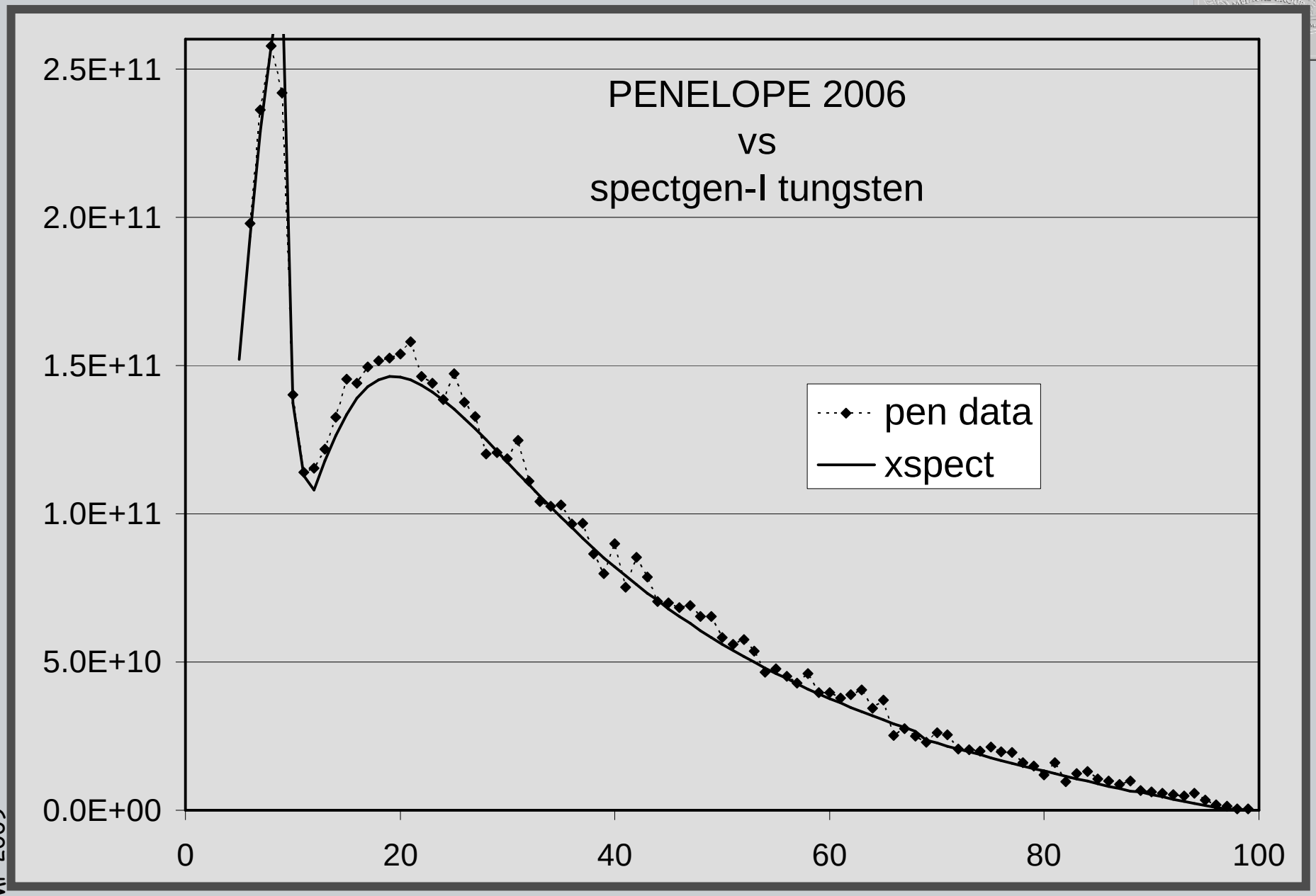

II – Primary spectrum attenuation

- XSPECT 'atten' script call
- Typically computed at object surface and detector surface.

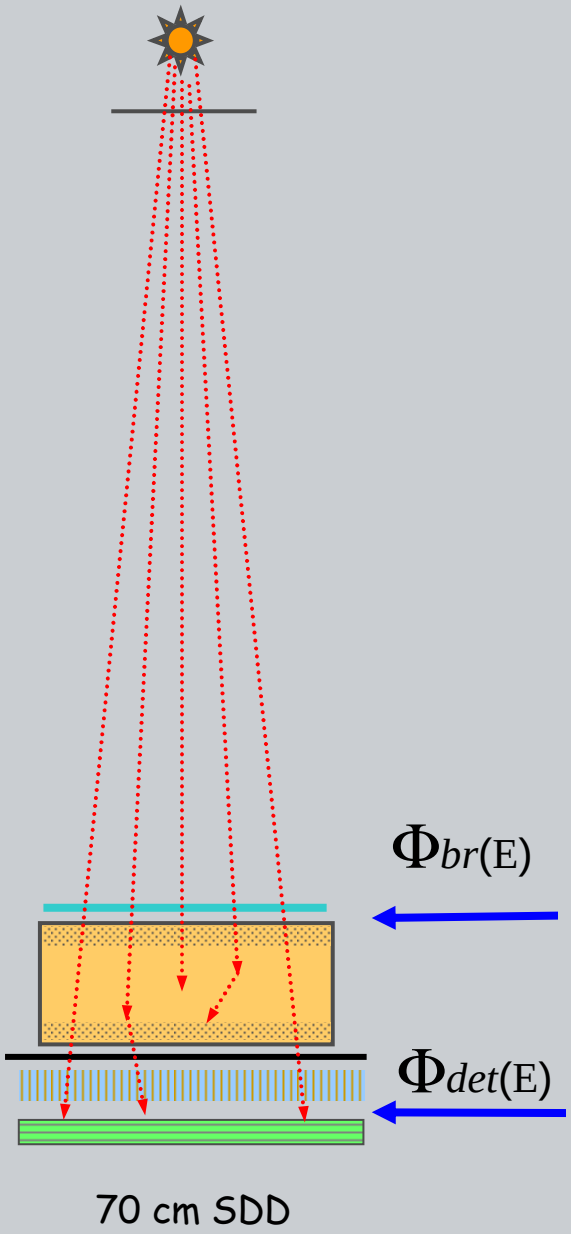

$\Phi_{br}(E)$ and $\Phi_{det}(E)$, Photons/cm2/mA-s

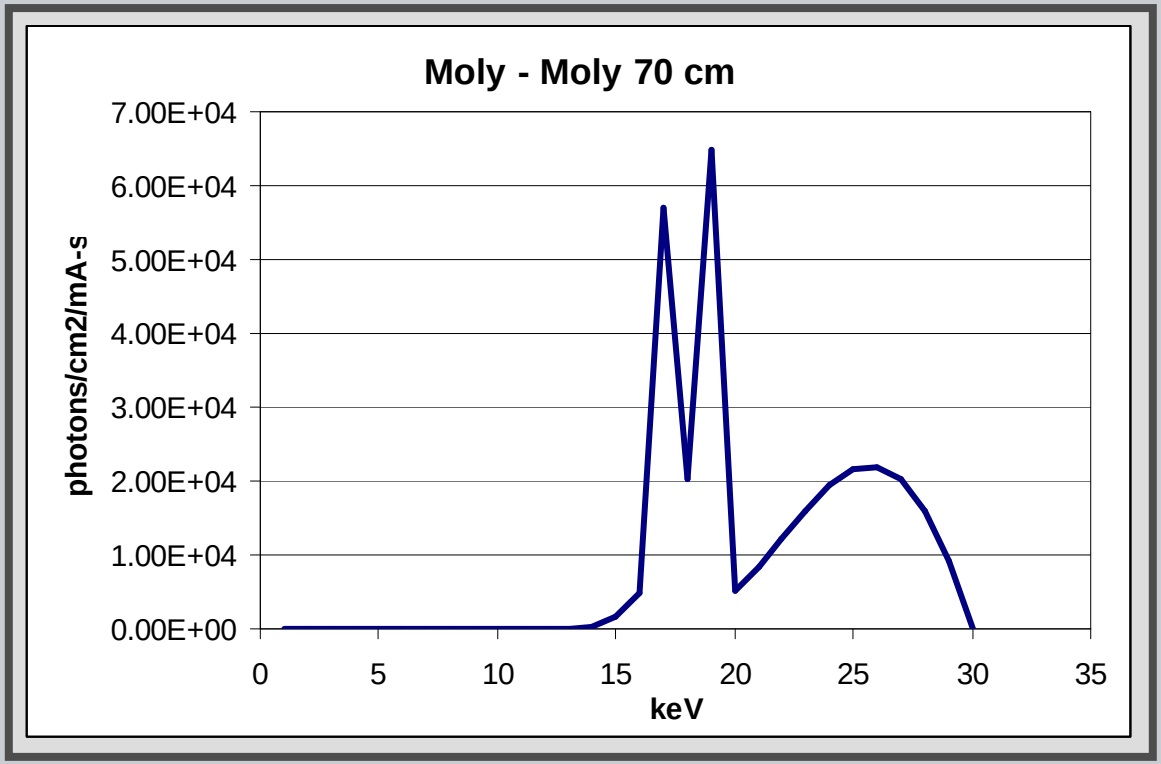

II – Spectral Attenuation

The XSPECT 'atten' procedure attenuates the x-ray spectral data for a specified list of material.

For a typical glass envelope tungsten tube;

```
> atten
  3
  glass_pyrex   .148
  oil           .300
  al_1100       .1
```

'atten' appends an attenuation history to the spectral data structure

---

No. of materials
Material1 thickness1
Material2 thickness2
. .

```
# spect_gen: 74  12.000  1 120.00
#   120   1.0000      0.0000
#    1   1  (unit flags)
#  Energy        #/mAs-sr-keV
    1.000         0.0000E+00
    2.000         0.0000E+00
   .
   .
    119.000       3.1155E+08
    120.000       0.0000E+00
#  Attenuation History:
#  4
# glass_pyrex       1.4800E-01
# oil               3.0000E-01
# al_1100           1.0000E-01
# al_1100           3.0000E-01
```

- A library of data files containing material composition in a standard format that is accessed by file name.
- 106 materials as of Jan 2004.
- The standardized data files are also used by the SKEPTIC Monte Carlo code (S. Wilderman) and the DETECT optical Monte Carlo code (A. Badano).

- line 1: no. of elements
- line 2: Z of each element
- line 3: either:
  - No. per molecule (int)
  - weight fraction (if < 1)
- line 4: density.
- line 5: Condensed or Gas
- line 6: Pressure for G

Parylene:

```
2
6 1
8 8
1.11
C

manufacturers data from
www.lebowcompany.com. Confirmed
at www.parylene.com. Density
varies depending on paraylene
type. Parylene N assumed due to
constant dielectric constant over
a wide range of temperatures
```

II – Exposure – mR (coulombs/kg)

- Exposure is determined by an XSPECT script procedure that integrates the product of the energy spectrum (photons/cm^2/keV) and the air energy absorption coefficient (gms/ cm^2) to estimate the energy absorbed per gram;

$$g = \int \Phi(E) \frac{\mu_{en}}{\rho} dE$$

- The energy absorbed per gram, g (ergs/gm), is then converted to exposure using a conversion factor of 33.97 Joules/Coulomb (i.e. eV/ion, Boutillon 1987);

$$X = g/(33.97 \times 10^4) \ C/kg$$

$$X = g/87.643 \text{ Roentgens}$$

II – Air energy absorption coef.

Tabulated air energy absorbtion data from NIST based on calculations by Seltzer (Radiation Research 136, 147; 1993) are interpolated using a log-log transformation.

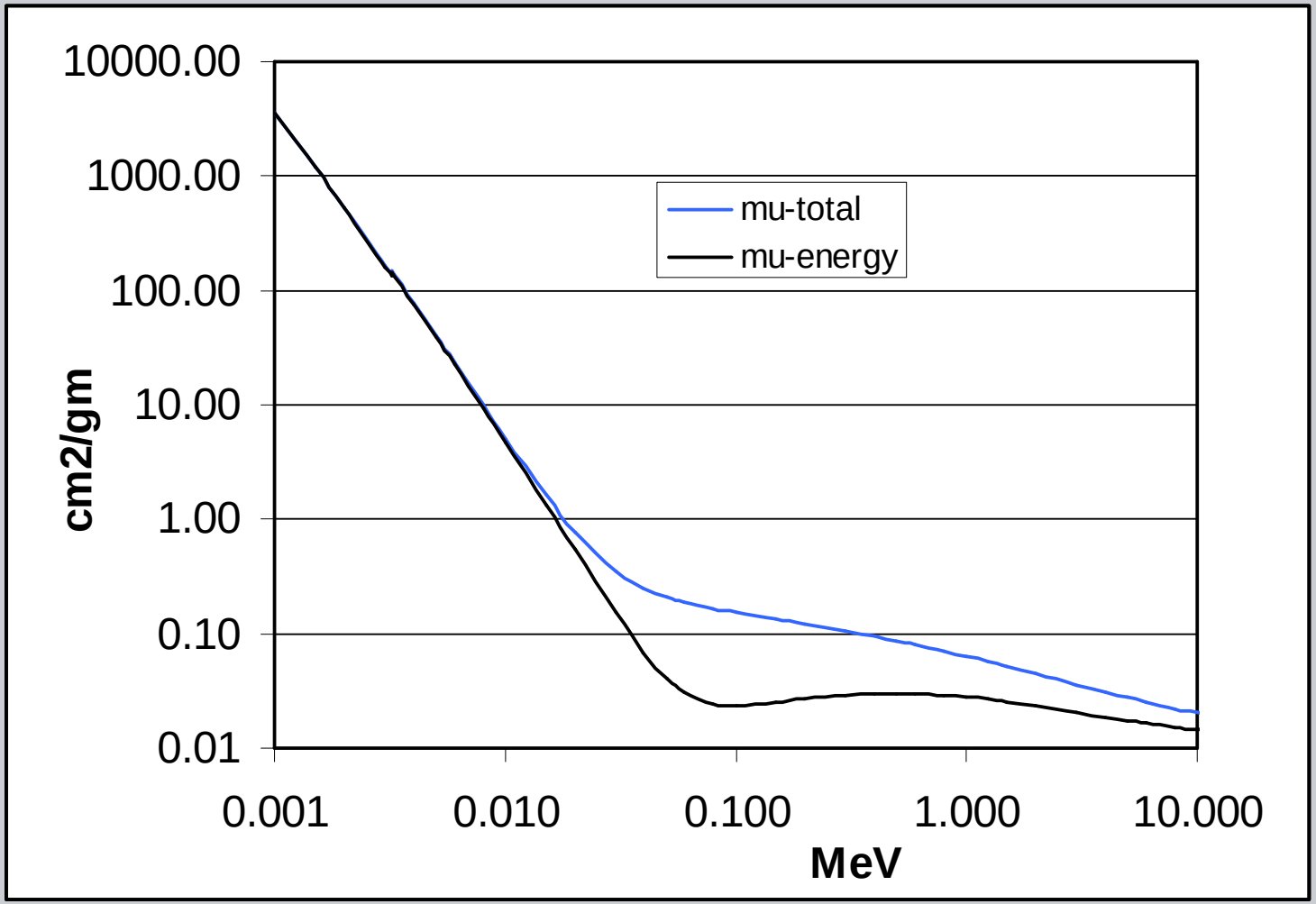

http://physics.nist.gov/PhysRefData

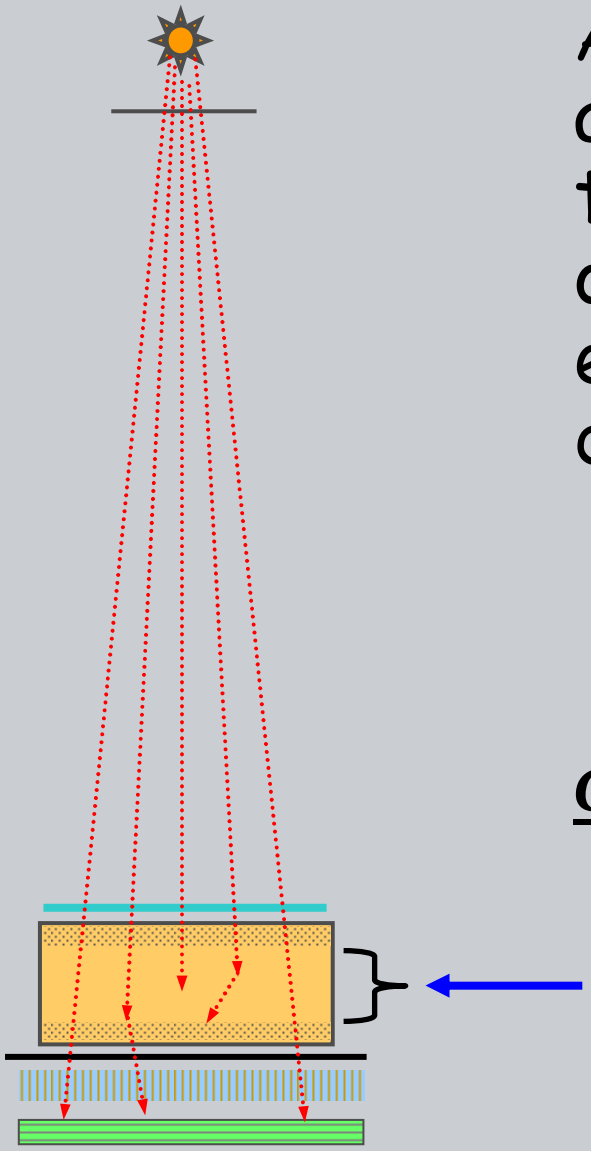

Absorbed dose is determined by an XSPECT script procedure that integrates the product of the energy spectrum and an energy dependant dose deposition function, ***G(E)*** ;

$$D = \int \Phi_{in}(E) G(E) dE$$

G(E) tables

- Monte Carlo computed tables.
- Must be computed for a specific object size using a geometry model that includes adjacent materials.
- Units of mGy/(photons/cm^2).

II – Object specific Dose tables

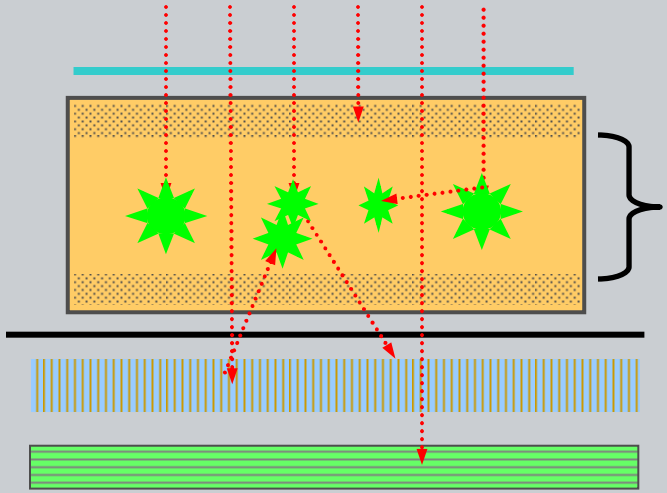

- G(E) is computed at 1 keV energy intervals using Monte Carlo simulation.
- For each energy, a many x-rays are tracked interaction by interaction through all materials.
- The energy depositions in the volume of interest are accumulated.
- The total energy binned is then normalized to the total number of photons/cm2 .

Breast phantom material

- BR12 50-50
- Excludes energy in top/bottom 5 mm

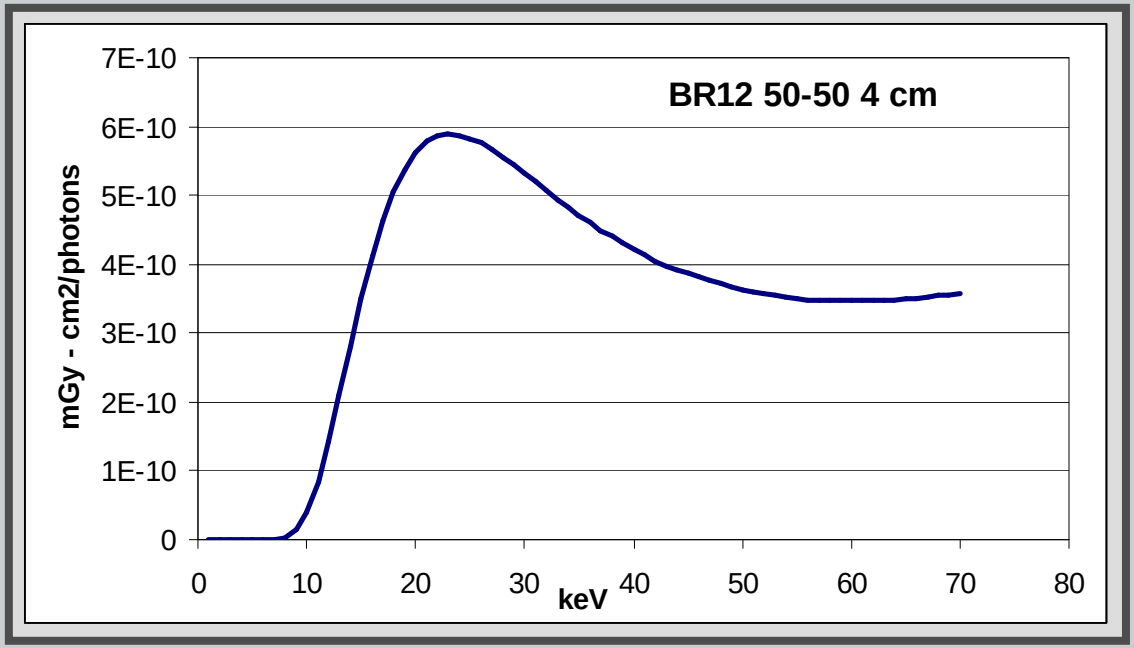

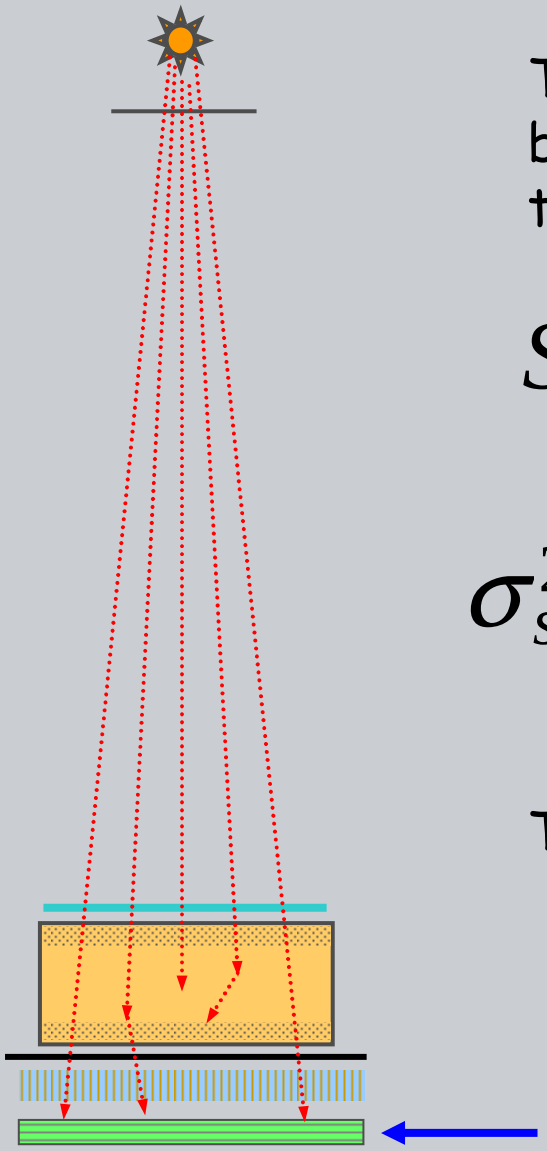

The detected signal and noise are determined by an XSPECT script procedure that integrates the product of the energy spectrum

$$S = A_p \bullet mA \bullet t \int \left(\varepsilon_s(E)\right) E \Phi_{\det}(E) dE$$

$$\sigma_s^2 = A_p \bullet mA \bullet t \int \left(\varepsilon_\sigma^2(E)\right) E^2 \Phi_{\det}(E) dE$$

Tabulated signal and noise transfer efficiencies

- Monte Carlo computed tables.
- Model includes all detector materials.
- Units of electrons/keV and $(\text{electrons/keV})^2$.

Detector efficiency tables are computed from the first and second moments of the normalized electron deposition probability function

moments

$$M_0(E) = \int P(n,E)dn$$

$$M_1(E) = \int nP(n,E)dn$$

$$M_2(E) = \int n^2 P(n,E)dn$$

$$\varepsilon_S(E) = \frac{(M_1/M_0)}{E}$$

$$\varepsilon_\sigma^2(E) = \frac{(M_2/M_0)}{E^2}$$

$$DQE_E = \frac{(\varepsilon_n(E))^2}{\varepsilon_\sigma^2(E)} = \frac{(M_1)^2}{M_2 M_0}$$

II – 250 micron Se Detector

Detector materials

50 nm	ITO	<== layer 1
25 μm	parylene	<== layer 2
250 μm	a-Se	<== layer 3
100 nm	ITO	<== layer 4
200 nm	Si3N4	<== layer 5
50 nm	Cr	<== layer 6
1.1 mm	glass_1737	<== layer 7

Monte Carlo computation of energy deposition

P(e,E)de

The normalized energy deposition probability function is computed for layer 3, a-Se

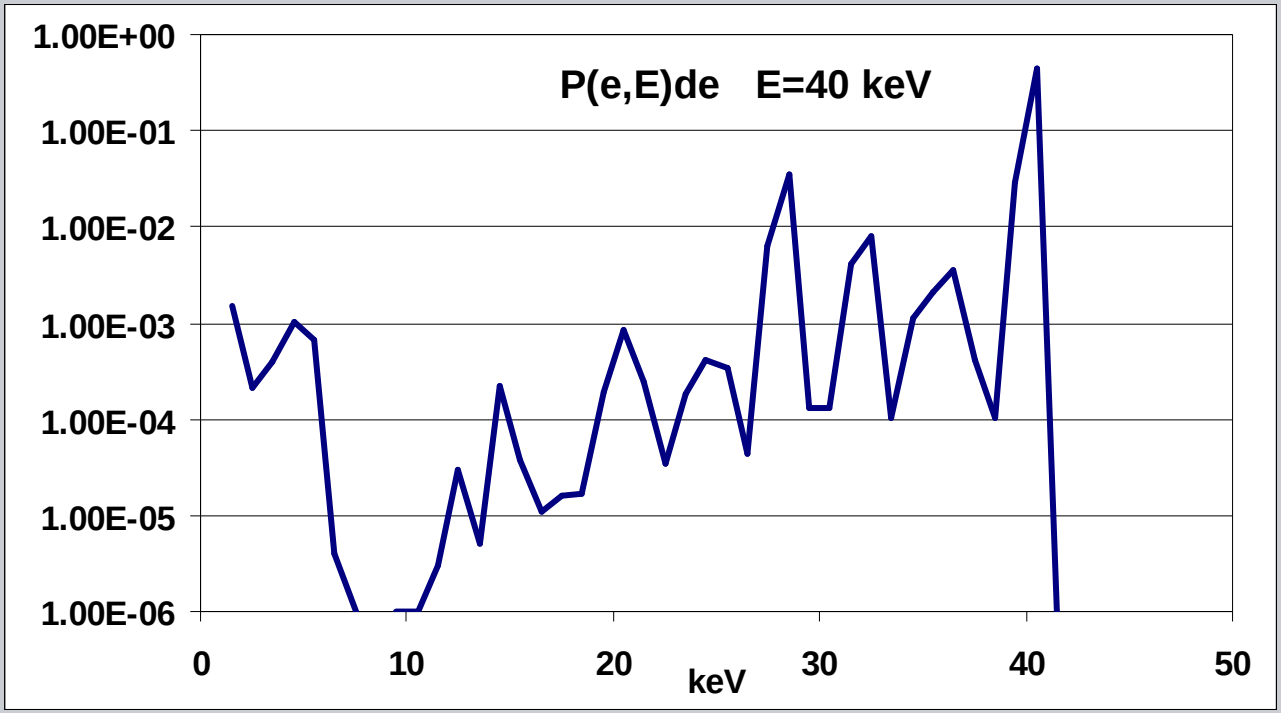

Electron production deduced from mean keV/e

The number of elections produced, $P(n,E)dE$ is computed as the integral of $P(n,e)\,P(e,E)de$

$P(n,e)\,de$ is a Poisson distibution function with mean n determinted from keV/e data.

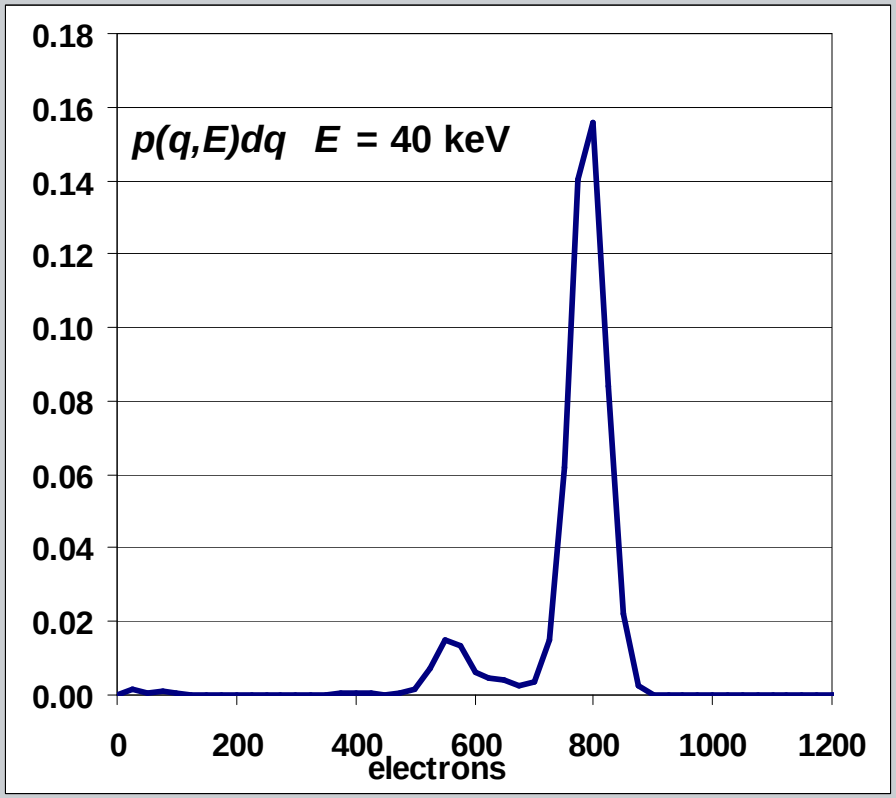

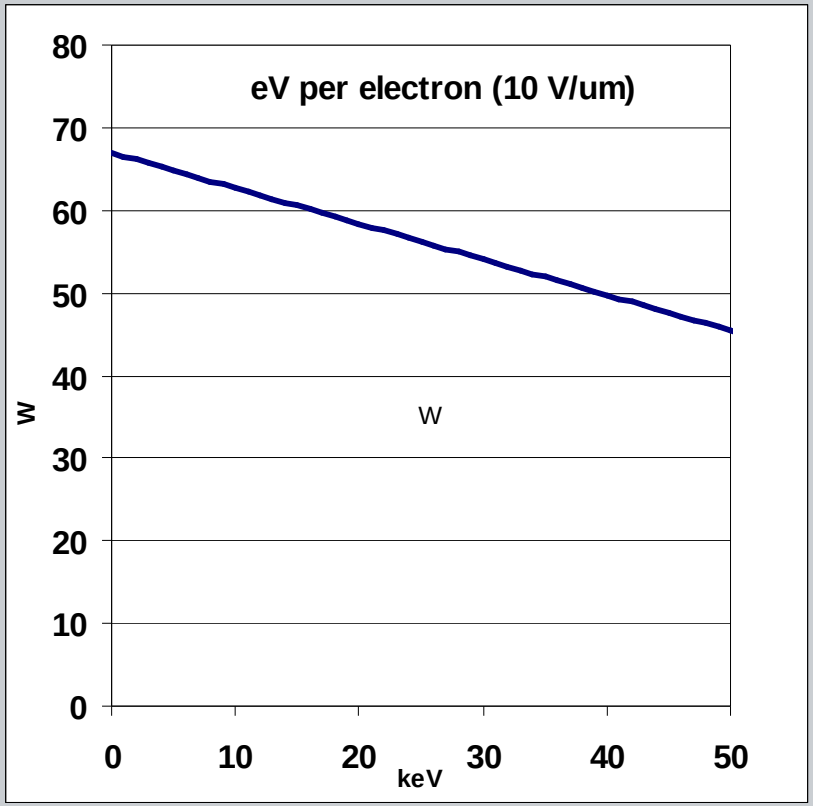

(see Blevis, Med.Phys.,1998)

II – Detector DQE(E)

The computed DQE(E) for monoenergetic x-rays is a useful description of detector performance but can not be used for broad spectrum simulations.

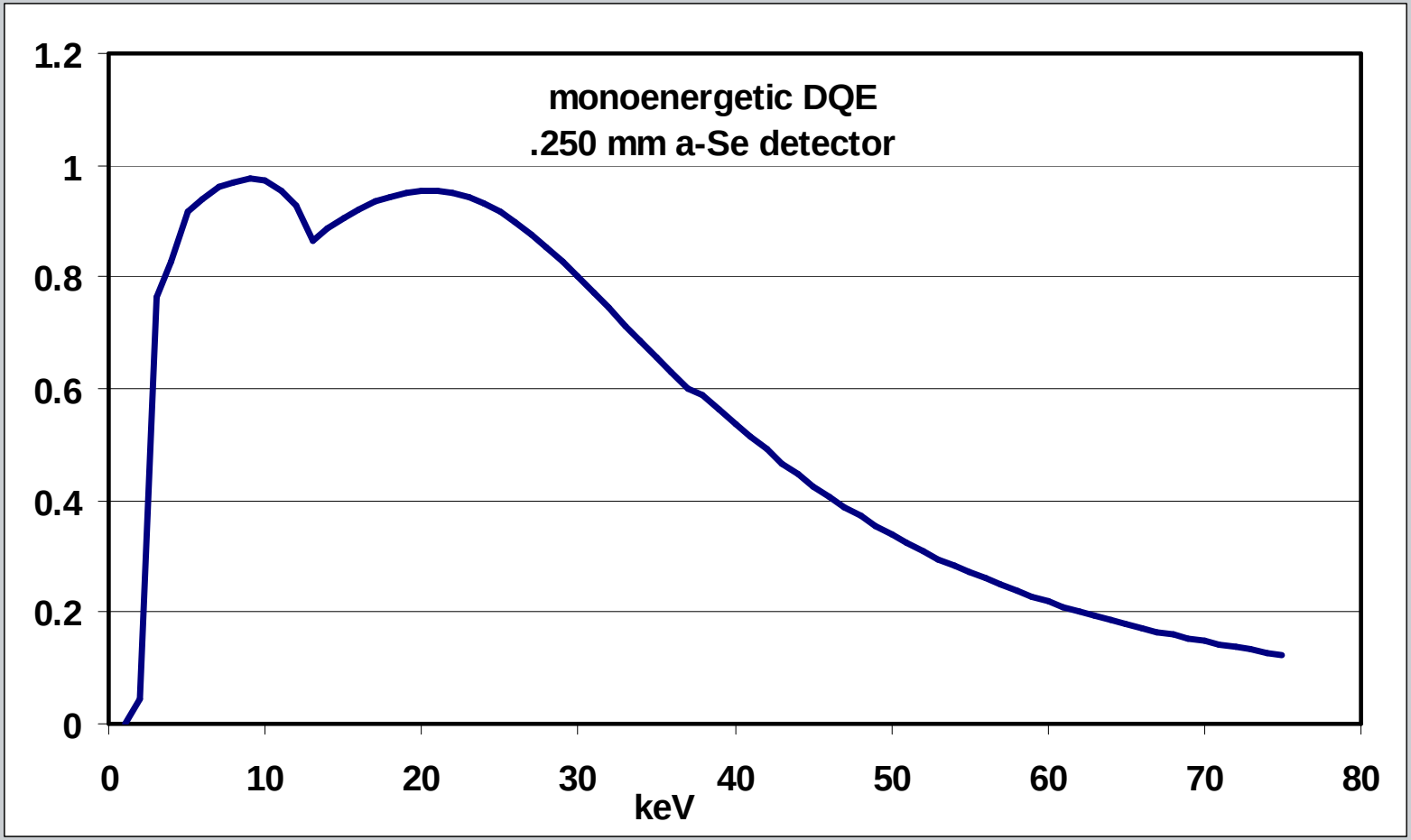

II – Relative Contrast

The relative contrast of a target structure is defined as the absolute signal difference between the target and the background divided by the background signal.

Relative Contrast

$$C_r = (St-Sb)/Sb$$

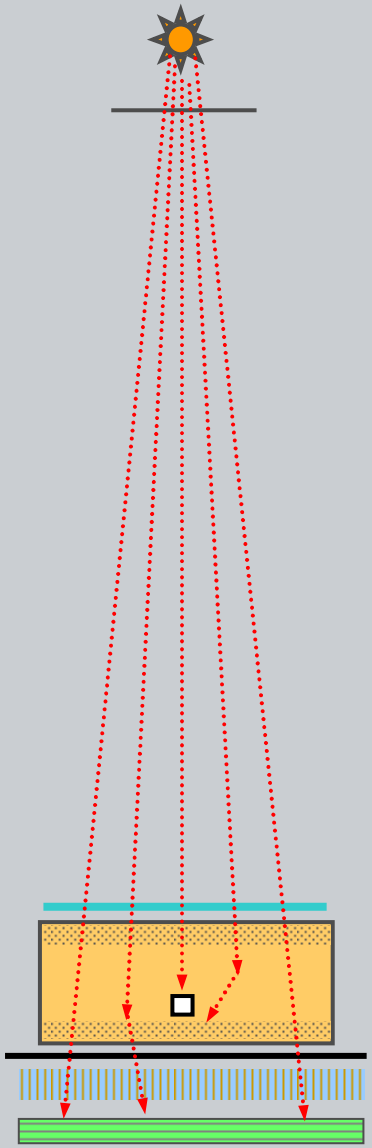

70 cm SDD

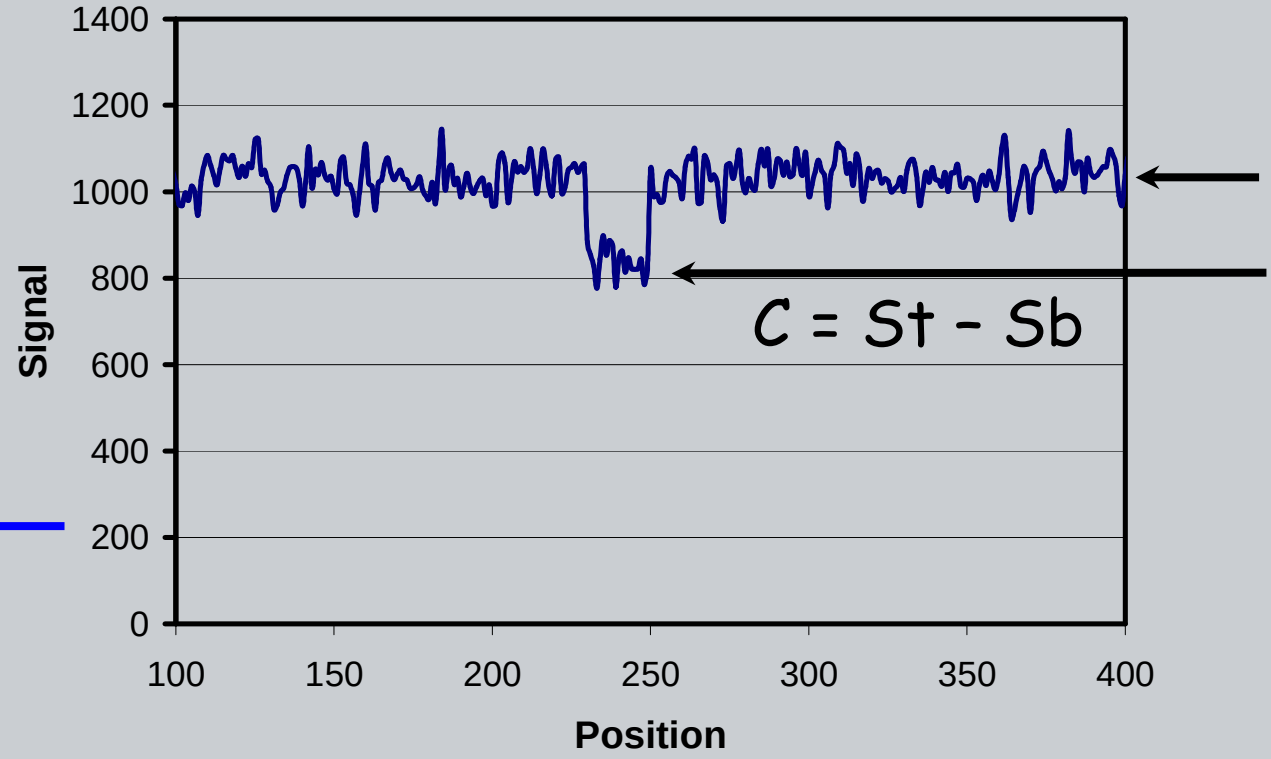

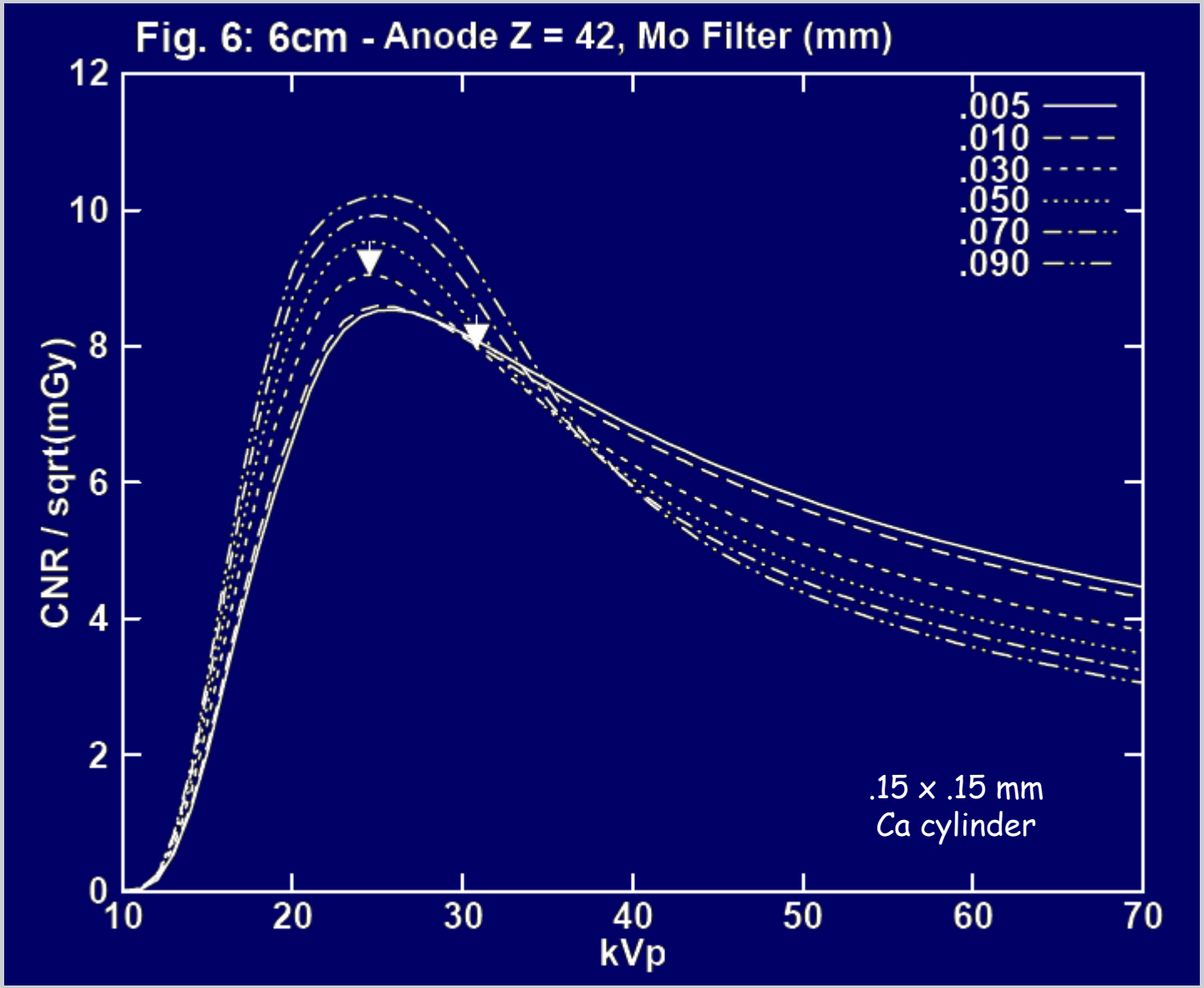

Flynn,Dodge, Peck.., SPIE 2003

II – Mammography technique optimization

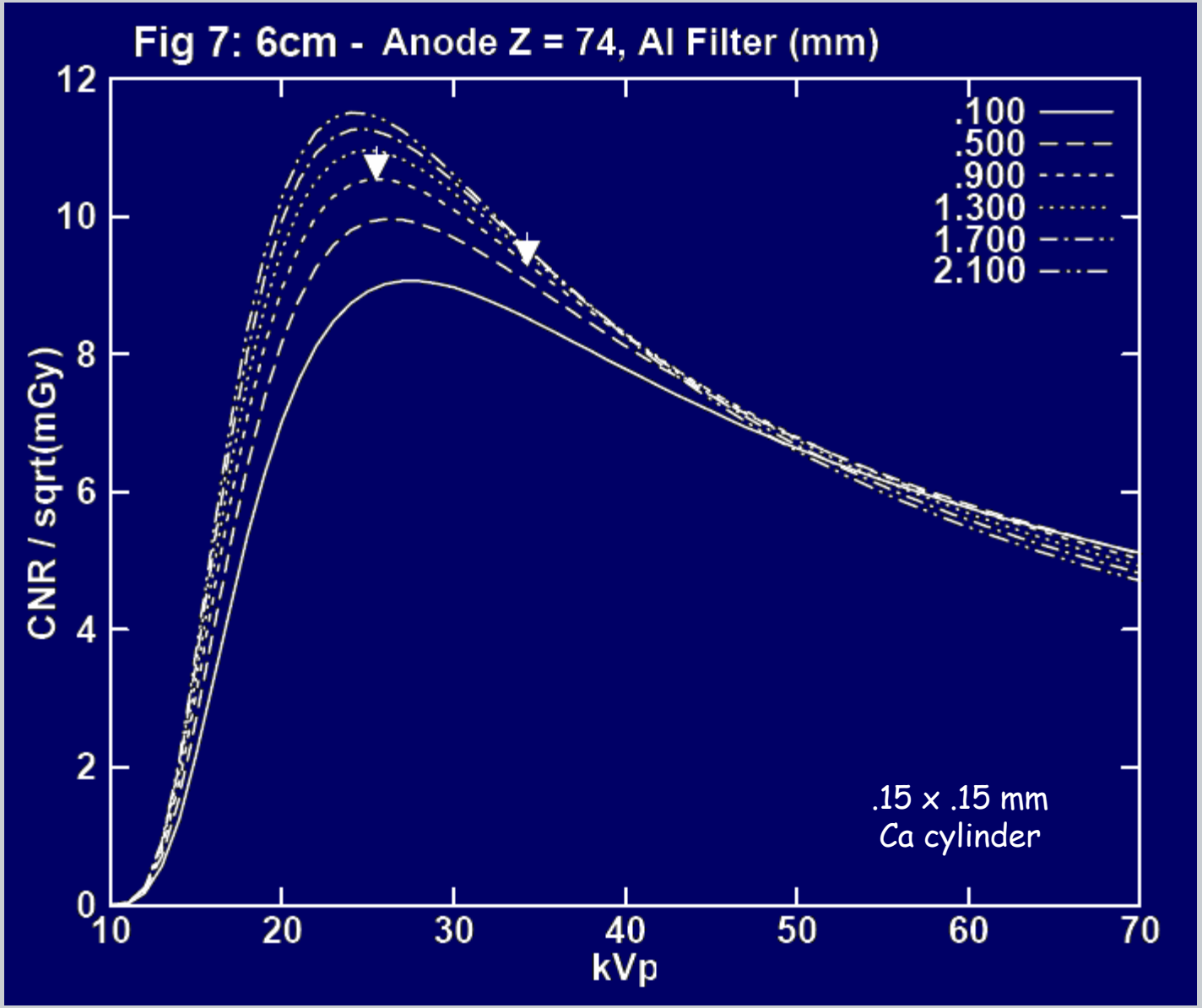

Flynn,Dodge, Peck.., SPIE 2003

II – Mammography technique optimization

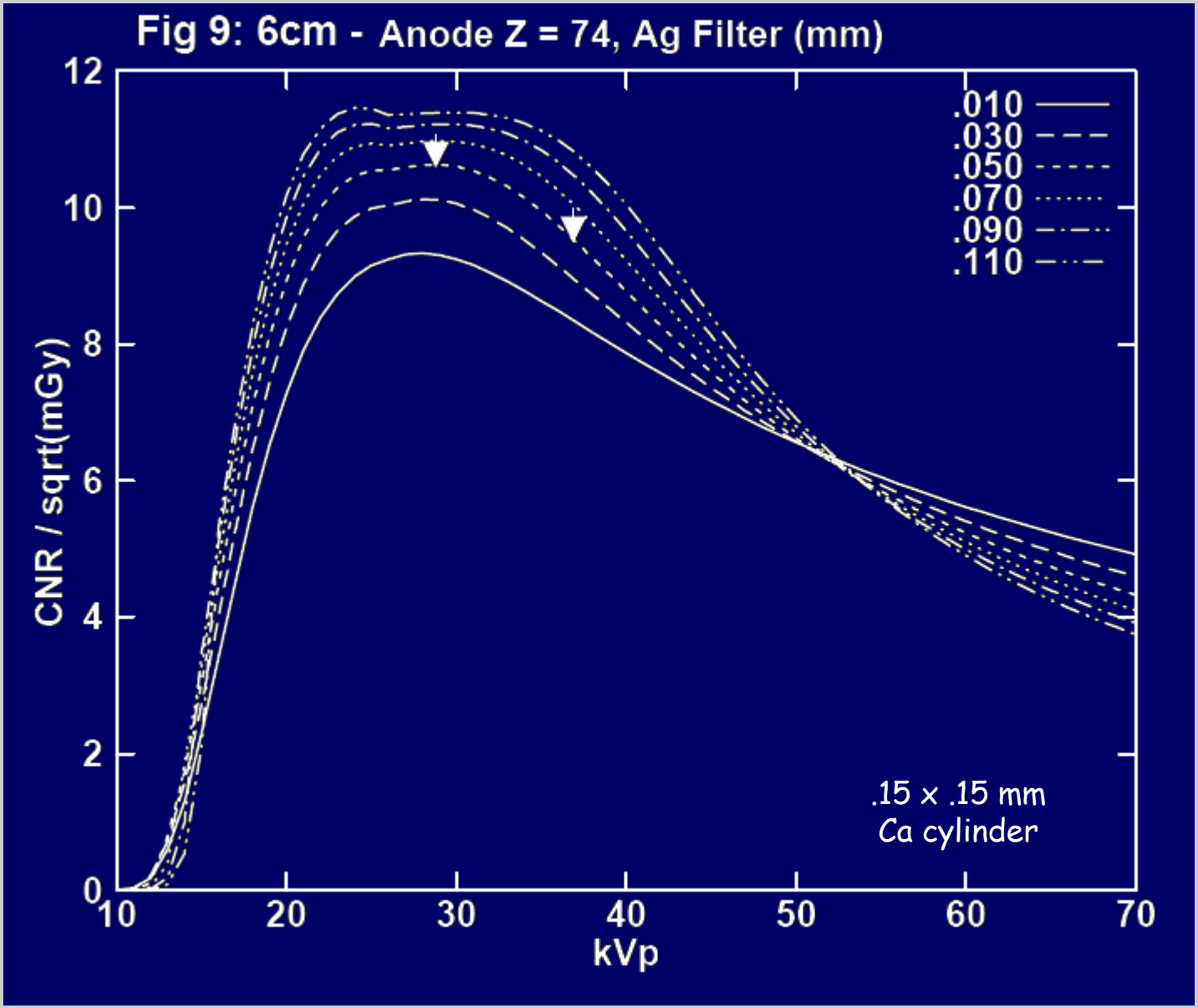

Flynn,Dodge, Peck.., SPIE 2003

Dose and mA-s for a constant CNR = 10

Maximum CNR

	mGy		mA-s		kVp	
Thickness	Mo/Mo	W/Sn	Mo/Mo	W/Sn	Mo/Mo	W/Sn
4 cm	0.33	0.35	53	34	24.0	22
6 cm	1.2	1.0	215	77	24.5	26
8 cm	4.7	2.6	1086	120	25.0	31

High kVp at .9 times max CNR

	mGy		mA-s		$kVp_{90\%}$	
Thickness	Mo/Mo	W/Sn	Mo/Mo	W/Sn	Mo/Mo	W/Sn
4 cm	0.4	0.43	21	14	31	30
6 cm	1.52	1.3	114	27	31	38
8 cm	5.7	3.2	435	62	33	42

- III -

Recent experimental reports confirm the use of W anode x-ray tubes for digital mammography, at least for selenium dDR detectors.

III – Recent experimental results

2006 - Clinical optimization of filters in direct a-Se FFDM System; N Uchiyama, N Moriyama, M Kitagawa et al; Proceedings 8th IWDM.

2006 - Beam optimization for digital mammography; M Williams, P Raghunathan, A Seibert et al; Proceedings 8th IWDM.

2006 - X-ray spectrum optimization of full-field digital mammography:Simulation and phantom study; P Bernhardt, T Mertelmeiet, M Hoheisel; Med Phys 33 (11).

2007 - Experimental investigation on the choice of the tungsten/rhodium anode/filter combination for an amorphous selenium-based digital mammography system; P Toroi, F Zanca, K Young et al; Eur Radiol 17

2008 - Effect of Anode/Filter Combination on the Dose and Image Quality of a Digital Mammography System Based on an Amorphous Selenium Detector; P Baldelli, N Phelan, G Egan; Proceedings 9th IWDM.

2008 - Effect of Using Tungsten-Anode X-Ray Tubes on Doseand Image Quality in Full-Field Digital Mammography; J Oduko, K Young, O Gundogdu et al; Proceedings 9th IWDM.

2008 - Optimizing the Target-Filter Combination in Digital Mammography in the Sense of Image Quality and Average Glandular Dose; M Varjonen, P Strommer; Proceedings 9th IWDM.

2009 - Comparison of Anode/Filter Combinations in Digital Mammography with Respect to the Average Glandular Dose; D Uhlenbrock, T Mertelmeier; Radiologie (Fortschr Röntgenstr) 181.

In 2007, Toroi reported experiments CNR and dose for Siemens Novation systems (a-Se):

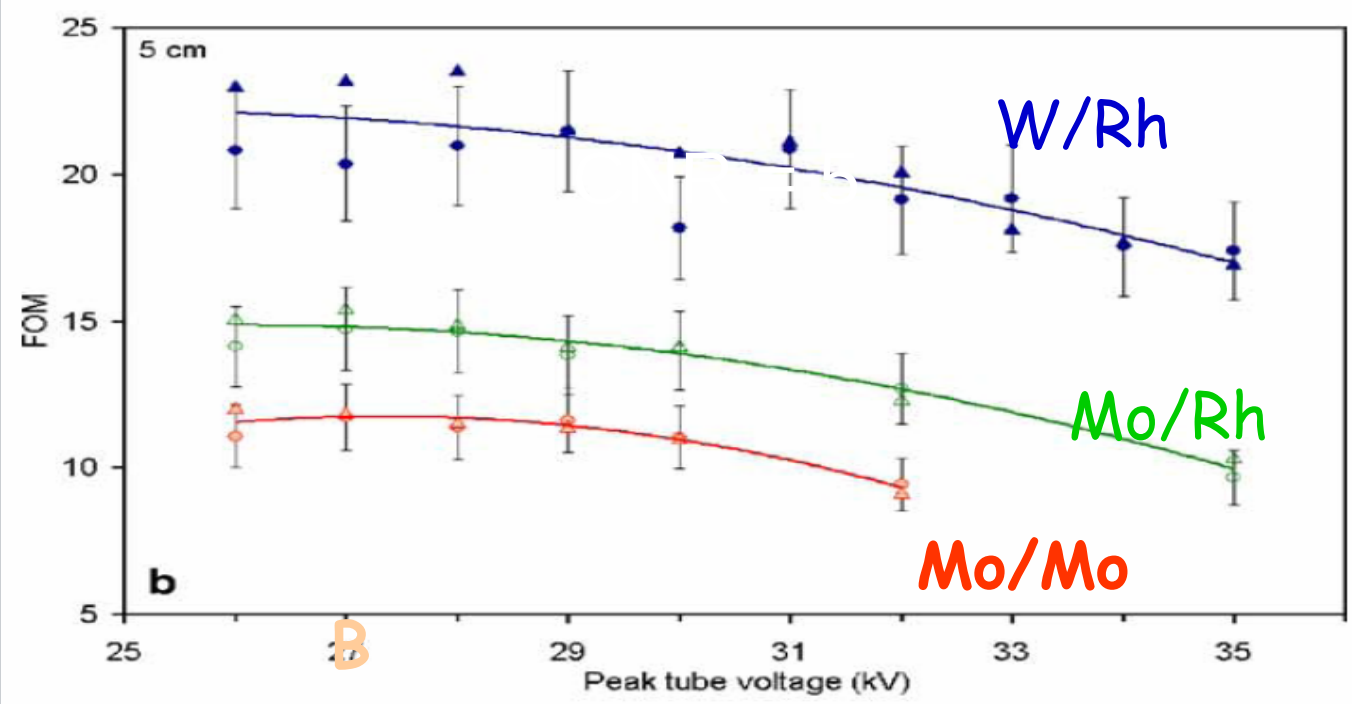

- CNR from PMMA/Al phantoms.
- Dose from computer program (Dance method)
- Two AEC modes.

" By using a W anode with a Rh(30 µm) filter, the same SDNR can be achieved with a significantly lower MGD than by using a Mo anode in combination with Mo(30 µm) or Rh(25 µm) filter."

Experimental investigation on the choice of the tungsten/rhodium anode/filter combination for an amorphous selenium-based digital mammography system; P Toroi, F Zanca, et al; Eur Radiol 17, 2007

In 2008, Bardelli compare image quality and dose on two Hologic Selenia systems (a-Se):

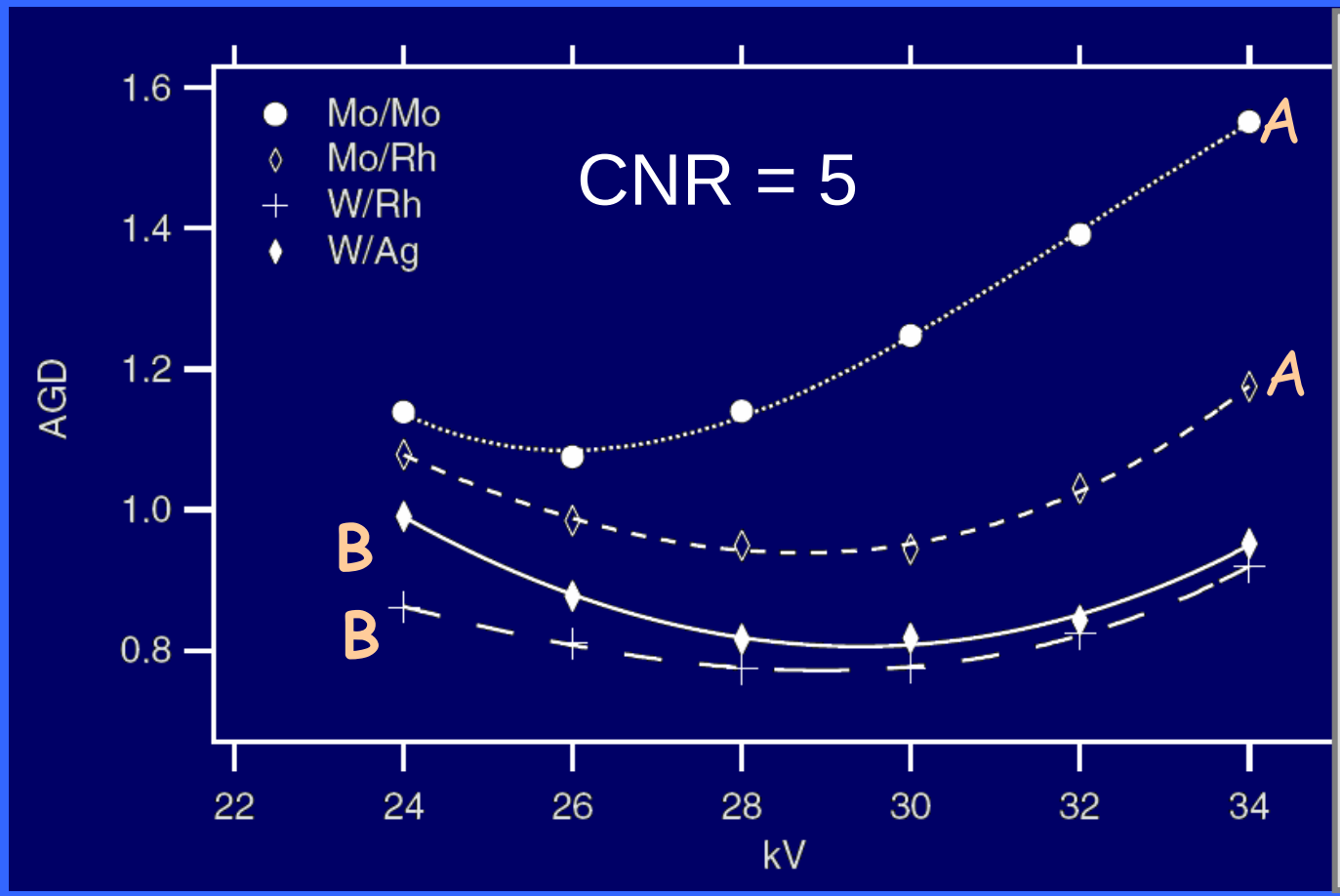

System A.
Mo/Mo(30mm)
Mo/Rh(35mm)
x-ray source

System B
W/Rh(50mm
W/Ag(50mm)
x-ray source

Effect of Anode/Filter combination on the dose and image quality of a digital mamm. system based on amorphous selenium detector; P Baldelli, N Phelan, G Egan, 9th IWDM 2009.

In Mar 2009, Uhlenbrock reported the average glandular dose (AGD) of 4867 digital mammograms (Siemens MAMMOMAT0, a-Se);

- 1793 done with Mo/Mo or Mo/Rh
- 2431 done with W/Rh

- AGD was 2.76 ± 1.31 mGy with Mo/Mo.
- AGD was 1.26 ± 0.44 mGy with W/Rh.
- Image quality was judged equivalent
- Conclusion:
  Applying a W/Rh beam quality permits the reduction of the patient dose by approximately 50% when using an FFDM system based on amorphous selenium.

Comparison of Anode/Filter Combinations in Digital Mammography with Respect to the Average Glandular Dose;
D Uhlenbrock, T Mertelmeier, Radiologie 181(3) Mar 2009.

In 2006, the DMIST group reported on beam optimization for five system.

System	Target	Filter	kV Range
Siemens	Mo, W	Mo,	23 – 35
Selenia	Mo	Mo,	23 – 39
Fischer	W	Al	28 – 37
GE	Mo, Rh	Mo,	24 – 32
Fuji	Mo	Rh	24 – 34

- "… in general, technique combinations resulting in higher energy beams resulted in higher FOM values, for nearly all breast types."
- "… the choice of target material and external filtration is more significant in determination of the overall FOM of a DM system than is choice of tube voltage."

More studies using CR and indirect DM are needed

Beam optimization for digital mammography; M Williams, P Raghunathan, A Seibert et al; Proceedings 8th IWDM, 2006.

COMMENT

- Contrast is highly dependent on image processing.
- Processing should always be optimized after FOM optimization.
- Spectral optimization should not be done without access to image processing parameters.

Se-TFT mammogram
Lorad (Hologic) Selenia
AAPM TG18-MM2

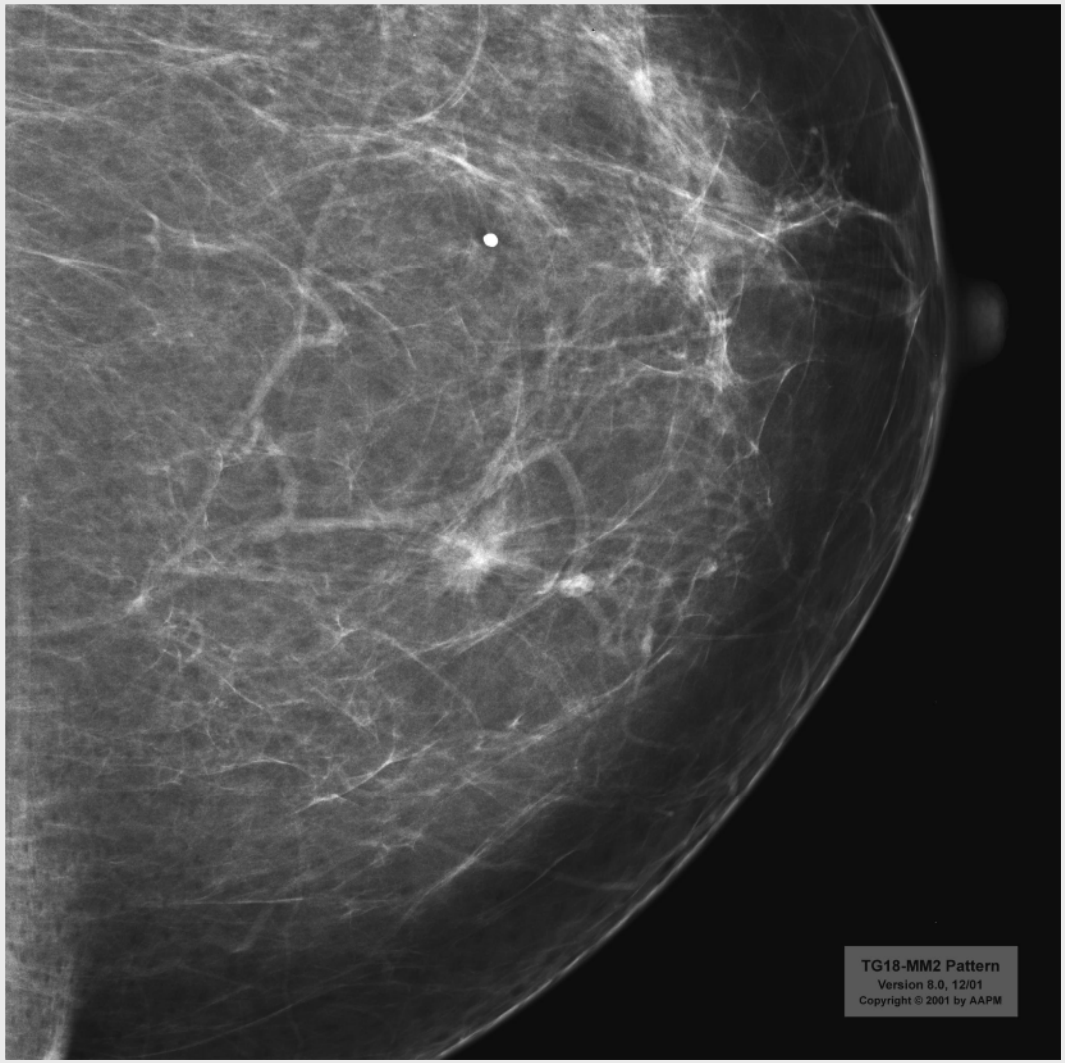

SUMMARY

- New a-Se digital mammography systems offer significant reductions in breast glandular dose for the same image quality (CNR)
- Similar improvements are likely to become available for other types of systems (iDR, CR)

Se-TFT mammogram
Lorad (Hologic) Selenia
AAPM TG18-MM2

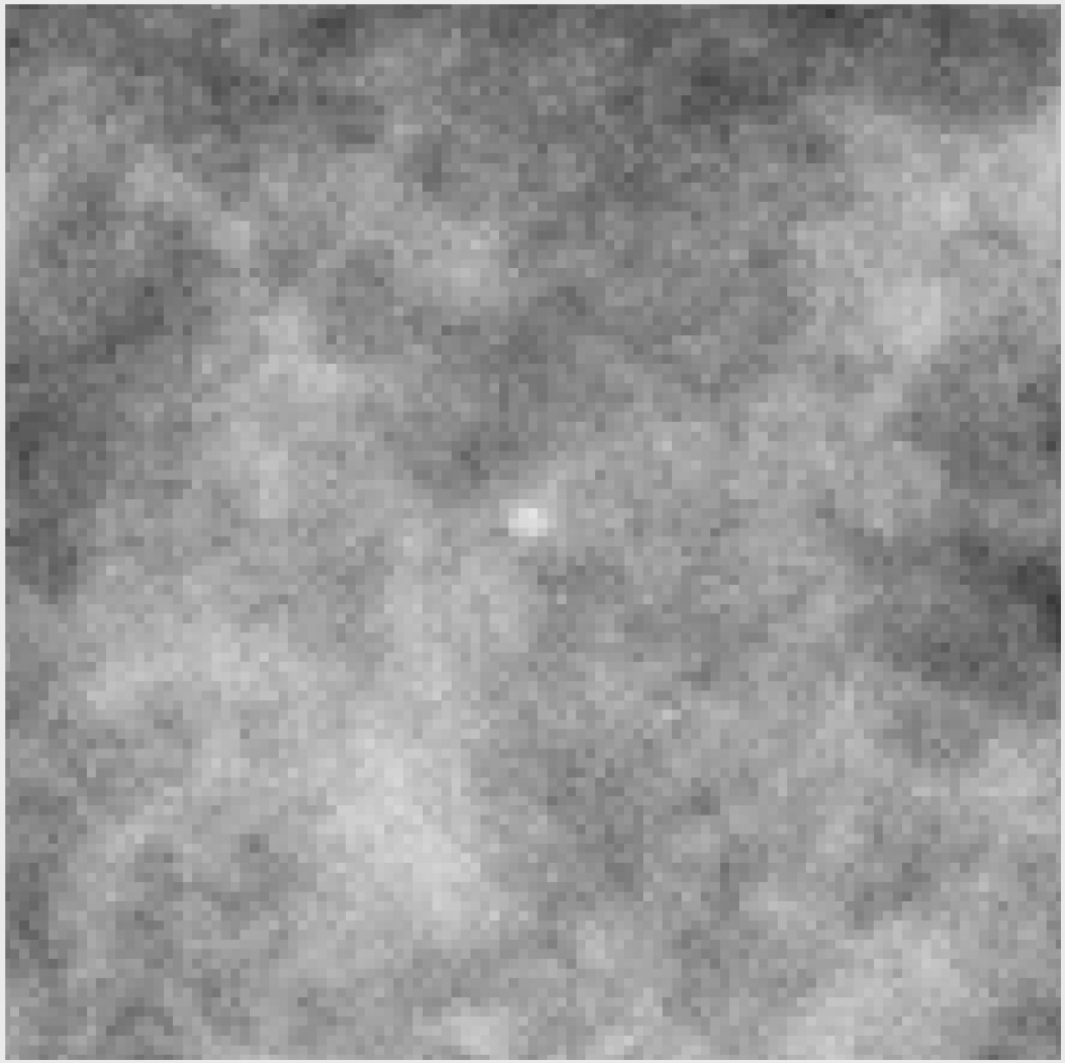

Questions?